Beamforming Optimization for Multiuser Two-Tier Networks

Youngmin Jeong, Tony Q. S. Quek, and Hyundong Shin

(Invited Paper)

Abstract: **With the incitation to reduce power consumption and the aggressive reuse of spectral resources, there is an inevitable trend towards the deployment of small-cell networks by decomposing a traditional single-tier network into a multi-tier network with very high throughput per network area. However, this cell size reduction increases the complexity of network operation and the severity of cross-tier interference. In this paper, we consider a downlink two-tier network comprising of a multiple-antenna macrocell base station and a single femtocell access point, each serving multiples users with a single antenna. In this scenario, we treat the following beamforming optimization problems: i) Total transmit power minimization problem; ii) mean-square error balancing problem; and iii) interference power minimization problem. In the presence of perfect channel state information (CSI), we formulate the optimization algorithms in a centralized manner and determine the optimal beamformers using standard convex optimization techniques. In addition, we propose semi-decentralized algorithms to overcome the drawback of centralized design by introducing the signal-to-leakage plus noise ratio criteria. Taking into account imperfect CSI for both centralized and semi-decentralized approaches, we also propose robust algorithms tailored by the worst-case design to mitigate the effect of channel uncertainty. Finally, numerical results are presented to validate our proposed algorithms.**

Index Terms: **Beamforming optimization, convex optimization, femtocell, imperfect channel state information, macrocell, power control, two-tier network.**

I. INTRODUCTION

The ever-growing need for wireless communications to improve coverage and provide high data rates leads to a substantial demand for new spectral resources and more effective transmission strategies [1]. Furthermore, energy consumption and electromagnetic pollution are becoming main societal and economical challenges that future communication systems have to tackle. An effective way to deploy such wireless networks is to decompose a traditional single-tier network into a multi-tier network with very high throughput per network area. As a result, a femtocell technology has recently received considerable attention for industrial standardization (see, e.g., [2]–[5] and reference therein). A femtocell network is a low-power and cost-effective communication system, which connects to the core network (e.g., macrocell network) via backhaul links.

Depending on the access control mechanism employed by the femtocells, the effect of cross-tier interference will differ significantly [3], [4]. In terms of access control, one can adopt open- or closed-access schemes in femtocell networks. The open-access scheme allows nearby macrocell users (MUs) to access the femtocell network freely by providing a cost-effective way to improve their capacity and coverage. In the closed-access scheme, only subscribed users are given authority to access the femtocell network. In particular, cross-tier interference for closed-access femtocell access points (FAPs) can significantly deteriorate the signal-to-interference-plus-noise ratio (SINR) at the MUs and macrocell base station (MBS) in the downlink and uplink scenarios, respectively. Therefore, interference management is one of the important challenges in femtocell networks [6]–[9].

Both centralized and distributed uplink power control algorithms were considered in [6] for single-antenna macrocell networks underlaid with single-antenna femtocell networks. Adopting an information-theoretical approach, the uplink achievable rate regions were derived in [7] for the MBS and FAP with interference cancellation in single-cell and multicell systems, respectively. The uplink capacity analysis and interference avoidance strategy were presented for a two-tier code-division multiple-access network [8] and the downlink coverage analysis was further extended to the multiple antenna case with zero-forcing precoder [9]. Simple transmit beamforming methods for FAPs were proposed in [10] to mitigate the cross-tier interference to the MU without any guaranteed quality of service (QoS). The interference avoidance exploiting the characteristics of orthogonal frequency-division multiple-access systems was used in [11] to manage the cross-tier interference between femtocells and macrocells. The downlink carrier selection and transmit power control were proposed in [12] as key techniques to manage the cross-tier interference for 3G systems. Despite the aforementioned contributions, the two-tier optimization accounting for the interference management and system complexity in femtocell networks has not been well studied. For example, the multiple-input multiple-output (MIMO) optimization for femtocell networks has not been well studied, especially accounting for the uncertainty of channel state information (CSI). The backhaul links between the macrocell and femtocell base stations are also likely to be (bandwidth) limited since they usually leverage on the user's broadband internet connection.

It is well-known that multiple antennas can be utilized to re-

Manuscript received December 11, 2010.

This work was supported by the National Research Foundation of Korea (NRF) grant funded by the Korea government (MEST) (No. 2011-0018071 and No. 2011-0001274).

Y. Jeong and H. Shin are with the Department of Electronics and Radio Engineering, Kyung Hee University, 1 Seocheon-dong, Giheung-gu, Yongin-si, Gyeonggi-do, 446-701 Korea, email: {yjeong, hshin}@khu.ac.kr.

T. Q. S. Quek is with the Institute for Infocomm Research, A*STAR, 1 Fusionopolis Way, #21-01 Connexis South Tower, Singapore 138632, email: qsquek@ieee.org.

alize the multiplexing gain, diversity gain, or antenna gain, thus enhancing the data rate, the error performance, or the SINR of wireless systems, respectively [13]–[17]. Particularly, in a multiuser or interference-limited scenario, there has been considerable research work that investigated the use of beamforming techniques to suppress interference as well as to satisfy the system QoS [18]–[24]. In [18] and [19], transmit power minimization and SINR balancing problems were studied through jointly optimizing the downlink beamformers and transmission power. The efficient algorithms were proposed in [20] for the minimum mean-square error (MMSE) balancing and aggregate mean-square error (MSE) minimization problems. In [21], the effect of imperfect CSI estimation on MIMO beamforming was addressed for CDMA systems. An alternative approach for designing transmit beamforming vectors based on the signal-to-leakage-plus-noise ratio (SLNR) was proposed in [22]–[24] for downlink multiuser MIMO channels.[1] Therefore, it is attractive to explore the potential of employing MIMO optimization in femtocell networks, accounting for imperfect CSI and the amount of coordination between inter-tier networks.

In this paper, we consider a downlink two-tier network comprising of a multiple-antenna MBS and a multiple-antenna FAP, each serving multiple users with a single antenna. In this scenario, we formulate the following beamforming optimization problems: i) Total transmit power minimization problem, ii) MSE balancing problem, and iii) interference power minimization problem to ensure that each QoS of the MUs and home users (HUs) can be satisfied. The main contributions of this paper are as follows.

- *Centralized and semi-decentralized designs*: Under perfect CSI, we solve the above optimization problems when a backhaul equipment is available. However, in practise, such a backhaul equipment may not always be present or feasible [25], [26]. To design the beamformers in a semi-decentralized manner, we decouple the beamforming and power allocation problems by first designing the beamformer in a distributed fashion using the SLNR criteria. The SLNR-based beamformer is attractive since it only requires the CSI from the transmitter to its own serving users and its victim users to which it causes interference. Next, we determine the power allocations at the MBS and FAP *locally* by exchanging only minimal information.
- *Robust design with imperfect CSI*: Due to the nature of wireless propagation environments and the latency in sharing of the CSI between the MBS and FAP, it is difficult to obtain perfect CSI of all the links. Therefore, using the concept of robust worst-case design [27]–[30], we further "practicalize" our centralized and semi-decentralized beamforming algorithms taking into account such CSI uncertainty.

The layout of this paper is as follows. In Section II, we present the system model of two-tier networks. Section III formulates the optimization problems assuming perfect CSI and the presence of a centralized network controller. In Section IV, we propose semi-decentralized design to solve the optimization problems with minimal exchange of information between the MBS and FAP. Section V extends our proposed centralized and semi-decentralized algorithms to robust counterparts in the presence of imperfect CSI. In Section VI, we provide some numerical results and finally, conclusion is drawn in Section VII.

[1]The co-channel interference is caused by all other users at a desired user, while the leakage refers to the interference generated by the signal intended for the desired user on the remaining users. Hence, the leakage indicates how much signal power is leaked into the other users [22].

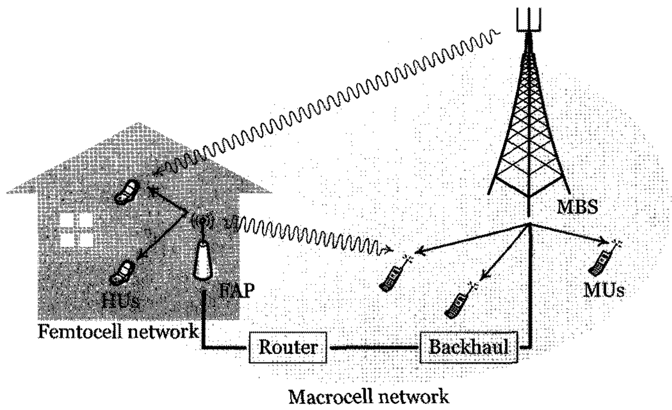

Fig. 1. Two-tier networks comprising of a single macrocell network and a single femtocell network. The blue lines indicate the desired links whereas the red lines indicate the cross-tier interference.

Notation: Throughout the paper, we shall use the following notation. Boldface upper- and lower-case letters denote matrices and column vectors, respectively. The superscripts T and $\dagger$ stand for the transpose and transpose conjugate, respectively. We use $\mathbb{C}$, $\mathbb{R}_+$, and $\mathbb{R}_{++}$ to denote the field of complex numbers and the sets of nonnegative real numbers and positive real numbers, respectively. We denote a vector with all one elements by $\mathbf{1}$ and an identity matrix by $\mathbf{I}$. The notations $|\cdot|$, $\|\cdot\|$, and $\|\cdot\|_{\mathrm{F}}$ denote the absolute value, the standard Euclidean norm, and the Frobenius norm, respectively. The trace operator of a square matrix is denoted by $\mathrm{tr}(\cdot)$. Finally, we use $\mathcal{CN}(\mu, \sigma^2)$ to denote a circularly symmetric complex Gaussian distribution with mean μ and variance σ^2.

II. SYSTEM MODEL

As illustrated in Fig. 1, we consider a downlink two-tier network where the MBS and FAP (transmitters) have N_{m} and N_{f} antennas, respectively. In particular, we consider the closed-access scheme whereby MBS and FAP transmissions occur simultaneously in a common frequency band with L MUs and K HUs. Each of the MUs and HUs is equipped with a single antenna. In this model, we are interested to serve the MUs while minimizing the amount of interference experienced at the MUs or maintaining the QoS of MUs.[2]

Let MU_l and HU_k denote the lth macrocell and kth home users where $l \in \mathcal{L} \triangleq \{1, 2, \cdots, L\}$ and $k \in \mathcal{K} \triangleq \{1, 2, \cdots, K\}$. Then, the received signals at MU_l and HU_k can be written as

$$y_{\mathrm{m},l} = \mathbf{g}_{\mathrm{m},l}^{\dagger}\mathbf{x}_{\mathrm{m}} + \mathbf{g}_{\mathrm{f},l}^{\dagger}\mathbf{x}_{\mathrm{f}} + z_{\mathrm{m},l} \quad (1)$$

$$y_{\mathrm{f},k} = \mathbf{h}_{\mathrm{f},k}^{\dagger}\mathbf{x}_{\mathrm{f}} + \mathbf{h}_{\mathrm{m},k}^{\dagger}\mathbf{x}_{\mathrm{m}} + z_{\mathrm{f},k} \quad (2)$$

[2]Our framework can be easily extended to the case of multiple MBSs and/or FAPs by adding the objective and constraint functions of each network in Sections III–V.

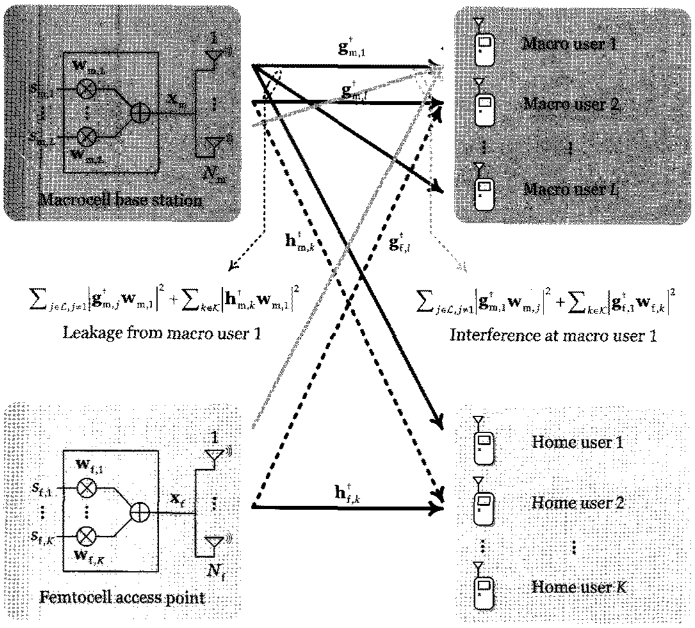

Fig. 2. Multiuser multiple-input single-output (MISO) femtocell network.

where $\mathbf{x}_{\mathrm{m}} \in \mathbb{C}^{N_{\mathrm{m}}\times 1}$ and $\mathbf{x}_{\mathrm{f}} \in \mathbb{C}^{N_{\mathrm{f}}\times 1}$ are the signal vectors transmitted from the MBS and FAP, respectively; $\mathbf{g}_{\mathrm{m},l}^{\dagger} \in \mathbb{C}^{1\times N_{\mathrm{m}}}$ and $\mathbf{h}_{\mathrm{m},k}^{\dagger} \in \mathbb{C}^{1\times N_{\mathrm{m}}}$ are the random channel vectors from the MBS to MU_l and HU_k, respectively; $\mathbf{g}_{\mathrm{f},l}^{\dagger} \in \mathbb{C}^{1\times N_{\mathrm{f}}}$ and $\mathbf{h}_{\mathrm{f},k}^{\dagger} \in \mathbb{C}^{1\times N_{\mathrm{f}}}$ are the random channel vectors from the FAP to MU_l and HU_k, respectively; and $z_{\mathrm{m},l} \sim \mathcal{CN}(0,\sigma_{\mathrm{m},l}^2)$ and $z_{\mathrm{f},k} \sim \mathcal{CN}(0,\sigma_{\mathrm{f},k}^2)$ are zero-mean complex additive white Gaussian noises.

At each transmitter (see Fig. 2), we consider a transmit beamforming strategy leading to transmitted signals of the MBS and FAP in forms of

$$\mathbf{x}_{\mathrm{m}} = \sum_{l\in\mathcal{L}} s_{\mathrm{m},l}\mathbf{w}_{\mathrm{m},l} \quad (3)$$

$$\mathbf{x}_{\mathrm{f}} = \sum_{k\in\mathcal{K}} s_{\mathrm{f},k}\mathbf{w}_{\mathrm{f},k} \quad (4)$$

where $\mathbf{w}_{\mathrm{m},l} \in \mathbb{C}^{N_{\mathrm{m}}\times 1}$ and $\mathbf{w}_{\mathrm{f},k} \in \mathbb{C}^{N_{\mathrm{f}}\times 1}$ are the transmit beamforming vectors for MU_l and HU_k, respectively; and $s_{\mathrm{m},l}$ and $s_{\mathrm{f},k}$ are the information signals for MU_l and HU_k with $\mathbb{E}\{|s_{\mathrm{m},l}|^2\} = \mathbb{E}\{|s_{\mathrm{f},k}|^2\} = 1$, respectively.

Let $\mathbf{W}_{\mathrm{m}} = [\mathbf{w}_{\mathrm{m},1}\ \mathbf{w}_{\mathrm{m},2}\ \cdots\ \mathbf{w}_{\mathrm{m},l}]$ and $\mathbf{W}_{\mathrm{f}} = [\mathbf{w}_{\mathrm{f},1}\ \mathbf{w}_{\mathrm{f},2}\ \cdots\ \mathbf{w}_{\mathrm{f},k}]$ for notational convenience. Then, the instantaneous SINRs at MU_l and HU_k can be expressed as

$$\mathsf{SINR}_{\mathrm{m},l}(\mathbf{W}_{\mathrm{m}},\mathbf{W}_{\mathrm{f}}) = \frac{|\mathbf{g}_{\mathrm{m},l}^{\dagger}\mathbf{w}_{\mathrm{m},l}|^2}{\sum_{j\in\mathcal{L},j\neq l}|\mathbf{g}_{\mathrm{m},l}^{\dagger}\mathbf{w}_{\mathrm{m},j}|^2 + \sum_{k\in\mathcal{K}}|\mathbf{g}_{\mathrm{f},l}^{\dagger}\mathbf{w}_{\mathrm{f},k}|^2 + \sigma_{\mathrm{m},l}^2} \quad (5)$$

$$\mathsf{SINR}_{\mathrm{f},k}(\mathbf{W}_{\mathrm{m}},\mathbf{W}_{\mathrm{f}}) = \frac{|\mathbf{h}_{\mathrm{f},k}^{\dagger}\mathbf{w}_{\mathrm{f},k}|^2}{\sum_{j\in\mathcal{K},j\neq k}|\mathbf{h}_{\mathrm{f},k}^{\dagger}\mathbf{w}_{\mathrm{f},j}|^2 + \sum_{l\in\mathcal{L}}|\mathbf{h}_{\mathrm{m},k}^{\dagger}\mathbf{w}_{\mathrm{m},l}|^2 + \sigma_{\mathrm{f},k}^2}, \quad (6)$$

respectively. We further introduce another figure of merit defined as the SLNR, which is attractive for semi-decentralized design of the beamforming vectors [22]–[24]. The instantaneous SLNRs of MU_l and HU_k are given by

$$\mathsf{SLNR}_{\mathrm{m},l}(\mathbf{W}_{\mathrm{m}}) = \frac{|\mathbf{g}_{\mathrm{m},l}^{\dagger}\mathbf{w}_{\mathrm{m},l}|^2}{\sum_{j\in\mathcal{L},j\neq l}|\mathbf{g}_{\mathrm{m},j}^{\dagger}\mathbf{w}_{\mathrm{m},l}|^2 + \sum_{k\in\mathcal{K}}|\mathbf{h}_{\mathrm{m},k}^{\dagger}\mathbf{w}_{\mathrm{m},l}|^2 + \sigma_{\mathrm{m},l}^2} \quad (7)$$

$$\mathsf{SLNR}_{\mathrm{f},k}(\mathbf{W}_{\mathrm{f}}) = \frac{|\mathbf{h}_{\mathrm{f},k}^{\dagger}\mathbf{w}_{\mathrm{f},k}|^2}{\sum_{j\in\mathcal{K},j\neq k}|\mathbf{h}_{\mathrm{f},j}^{\dagger}\mathbf{w}_{\mathrm{f},k}|^2 + \sum_{l\in\mathcal{L}}|\mathbf{g}_{\mathrm{f},l}^{\dagger}\mathbf{w}_{\mathrm{f},k}|^2 + \sigma_{\mathrm{f},k}^2}. \quad (8)$$

Assuming that all the receivers employ a linear MMSE filter for estimating their corresponding information sequences, we have a one-to-one relationship between the MSE and SINR as follows (see, e.g., [13], [20])

$$\mathsf{MSE}_{\mathrm{m},l}(\mathbf{W}_{\mathrm{m}},\mathbf{W}_{\mathrm{f}}) = \frac{1}{1+\mathsf{SINR}_{\mathrm{m},l}(\mathbf{W}_{\mathrm{m}},\mathbf{W}_{\mathrm{f}})} \quad (9)$$

$$\mathsf{MSE}_{\mathrm{f},k}(\mathbf{W}_{\mathrm{m}},\mathbf{W}_{\mathrm{f}}) = \frac{1}{1+\mathsf{SINR}_{\mathrm{f},k}(\mathbf{W}_{\mathrm{m}},\mathbf{W}_{\mathrm{f}})}. \quad (10)$$

The MSE measure is an important performance metric that quantifies how accurately each individual transmit information sequence can be recovered from the degenerate output sequence. Moreover, the relation between the mutual information and MMSE gives the information-theoretic point about limitation of Gaussian channels [31].

III. Centralized Design

Assuming perfect global CSI between two networks via backhaul links, we first formulate the centralized optimization problems using the MSEs in (9) and (10) as QoS measures.

A. Transmit Power Minimization Problem

Since transmission power is an important resource in wireless communications that is directly related to a network lifetime, it is crucial to minimize the average transmitted power while maintaining QoS constraints from the system level perspective [18]. Moreover, there is an increasing trend to limit the average transmission power due to radio pollution, global CO_2 emission, and greenhouse effects [32]. Thus, regulatory agencies will limit the total transmission power so as to reduce network interference between the MBS and FAP subject to QoS requirements at the MUs and HUs. Here, our design goal is to optimize the beamforming matrices $\mathbf{W}_{\mathrm{m}}$ and $\mathbf{W}_{\mathrm{f}}$ such that the total transmission power is minimized while constraining the MSE at each user to be below some maximum acceptable levels. Specifically, we have the following problem formulation.

$$\mathcal{P}_{\mathrm{tp}}: \begin{cases} \min\limits_{\mathbf{W}_{\mathrm{m}},\mathbf{W}_{\mathrm{f}}} & \|\mathbf{W}_{\mathrm{m}}\|_{\mathrm{F}}^2 + \|\mathbf{W}_{\mathrm{f}}\|_{\mathrm{F}}^2 \\ \text{s.t.} & \mathsf{MSE}_{\mathrm{m},l}(\mathbf{W}_{\mathrm{m}},\mathbf{W}_{\mathrm{f}}) \le \varepsilon_{\mathrm{m},l},\ \forall l\in\mathcal{L} \\ & \mathsf{MSE}_{\mathrm{f},k}(\mathbf{W}_{\mathrm{m}},\mathbf{W}_{\mathrm{f}}) \le \varepsilon_{\mathrm{f},k},\ \forall k\in\mathcal{K} \end{cases} \quad (11)$$

where $\mathcal{P}_{\mathrm{tp}}$ in (11) can be cast as (12), shown at the top of the next page, which is a second-order cone program (SOCP).

$$\mathcal{P}_{\rm tp}:\begin{cases}\min\limits_{\mathbf{W}_{\rm m},\mathbf{W}_{\rm f}} & \|\mathbf{W}_{\rm m}\|_{\rm F}^2+\|\mathbf{W}_{\rm f}\|_{\rm F}^2\\ \text{s.t.} & \frac{\Re\{\mathbf{g}_{{\rm m},l}^{\dagger}\mathbf{w}_{{\rm m},l}\}}{\sqrt{\sum_{j\in\mathcal{L},j\neq l}|\mathbf{g}_{{\rm m},l}^{\dagger}\mathbf{w}_{{\rm m},j}|^2+\sum_{k\in\mathcal{K}}|\mathbf{g}_{{\rm f},l}^{\dagger}\mathbf{w}_{{\rm f},k}|^2+\sigma_{{\rm m},l}^2}}\geq\sqrt{\frac{1}{\varepsilon_{{\rm m},l}}-1},\ \forall l\in\mathcal{L}\\ & \frac{\Re\{\mathbf{h}_{{\rm f},k}^{\dagger}\mathbf{w}_{{\rm f},k}\}}{\sqrt{\sum_{j\in\mathcal{K},j\neq k}|\mathbf{h}_{{\rm f},k}^{\dagger}\mathbf{w}_{{\rm f},j}|^2+\sum_{l\in\mathcal{L}}|\mathbf{h}_{{\rm m},k}^{\dagger}\mathbf{w}_{{\rm m},l}|^2+\sigma_{{\rm f},k}^2}}\geq\sqrt{\frac{1}{\varepsilon_{{\rm f},k}}-1},\ \forall k\in\mathcal{K}\end{cases}\tag{12}$$

Remark 1: Since the angular rotation of the beamforming vectors do not affect the constraints, we confine the solutions for $\mathcal{P}_{\rm tp}$ such that each of $\mathbf{g}_{{\rm m},l}^{\dagger}\mathbf{w}_{{\rm m},l}$ and $\mathbf{h}_{{\rm f},k}^{\dagger}\mathbf{w}_{{\rm f},k}$ has a nonnegative real part and a zero imaginary part [19].

B. MSE Balancing Problem

To ensure fairness between the HUs, we can optimize the beamformers such that the ratio of $\mathsf{MSE}_{{\rm f},k}/\varepsilon_{{\rm f},k}$ is balanced among all the HUs. The weight $\varepsilon_{{\rm f},k}$ are used to prioritize different HUs based on their QoS or latency requirements. Such an approach will ensure that all HUs satisfy their QoS similarly despite their different interference conditions due to fading or proximity of the macrocell system. Although we formulate the MSE balancing problem for the femtocell system in the following, we can also similarly formulate the MSE balancing problem for the macrocell system. Here, our design goal is to optimize the beamforming matrices $\mathbf{W}_{\rm m}$ and $\mathbf{W}_{\rm f}$ such that the maximum normalized MSE of HUs is minimized, while constraining the MSEs of MUs for their QoS guarantees as well as individual transmit powers of the MBS and FAP. Specifically, we have the following problem formulation.

$$\mathcal{P}_{\rm mse}:\begin{cases}\min\limits_{\mathbf{W}_{\rm m},\mathbf{W}_{\rm f}} & \max_{k\in\mathcal{K}}\varepsilon_{{\rm f},k}^{-1}\mathsf{MSE}_{{\rm f},k}(\mathbf{W}_{\rm m},\mathbf{W}_{\rm f})\\ \text{s.t.} & \mathsf{MSE}_{{\rm m},l}(\mathbf{W}_{\rm m},\mathbf{W}_{\rm f})\leq\varepsilon_{{\rm m},l},\quad\forall l\in\mathcal{L}\\ & \|\mathbf{W}_{\rm m}\|_{\rm F}^2\leq P_{\max,{\rm m}}\\ & \|\mathbf{W}_{\rm f}\|_{\rm F}^2\leq P_{\max,{\rm f}}\end{cases}\tag{13}$$

and by introducing a slack variable $\tau\in\mathbb{R}_{+}$, $\mathcal{P}_{\rm mse}$ can be equivalently written as

$$\mathcal{P}_{\rm mse}:\begin{cases}\min\limits_{\mathbf{W}_{\rm m},\mathbf{W}_{\rm f},\tau} & \tau\\ \text{s.t.} & \mathsf{MSE}_{{\rm f},k}(\mathbf{W}_{\rm m},\mathbf{W}_{\rm f})\leq\tau\varepsilon_{{\rm f},k},\quad\forall k\in\mathcal{K}\\ & \mathsf{MSE}_{{\rm m},l}(\mathbf{W}_{\rm m},\mathbf{W}_{\rm f})\leq\varepsilon_{{\rm m},l},\quad\forall l\in\mathcal{L}\\ & \|\mathbf{W}_{\rm m}\|_{\rm F}^2\leq P_{\max,{\rm m}}\\ & \|\mathbf{W}_{\rm f}\|_{\rm F}^2\leq P_{\max,{\rm f}}.\end{cases}\tag{14}$$

Table 1. Algorithm to solve $\mathcal{P}_{\rm mse}$.

1. Initialize $\tau_{\min}$ and $\tau_{\max}$ such that $\tau_{\min}\leq\tau^*\leq\tau_{\max}$ and set tolerance $\delta\in\mathbb{R}_{++}$.
2. Solve the convex feasibility problem $\mathcal{P}_{\rm mse}(\tau)$ by fixing $\tau=(\tau_{\max}+\tau_{\min})/2$.
3. If $\mathcal{P}_{\rm mse}(\tau)$ is feasible, then set $\tau_{\max}=\tau$ else set $\tau_{\min}=\tau$.
4. Stop if the gap $(\tau_{\max}-\tau_{\min})$ is less than the tolerance δ. Go to Step 1 otherwise.
5. Output $\mathbf{W}_{\rm m}^*$ and $\mathbf{W}_{\rm f}^*$ obtained from Step 2.

Unfortunately, since the first constraint in (14) is non-convex [19], $\mathcal{P}_{\rm mse}$ is not a convex optimization problem. However, for a given τ, $\mathcal{P}_{\rm mse}(\tau)$ becomes a convex feasibility problem as (15), shown at the bottom of the page.

Remark 2: Since the feasible sets are quasi-convex, we can solve $\mathcal{P}_{\rm mse}$ efficiently through a sequence of convex feasibility problems using the bisection method [33], [34]. The procedure is summarized in the Table 1.

Remark 3: The bisection method requires $\log_2\left(\frac{\tau_{\max}-\tau_{\min}}{\delta}\right)$ iterations to find the optimal value τ^* [33]. It is important that the interval range should contain the optimal solution. In our case, we set $\tau_{\max}$ to the unit transmit beamforming vectors and only need to choose $\tau_{\min}$ properly.

C. Network Interference Minimization Problem

Due to the broadcast nature of wireless transmission and spectrum underlay, the coexistence of macrocell and femtocell networks inevitably degrades the reception quality of their respective links by creating interference at their respective receivers. Therefore, we need to minimize the network interference level while the QoS is satisfied at each of the MUs and HUs. In this way, the system designer can further deploy additional underlay systems to reuse the same spectrum as long as the network interference level is tolerable. Here, our design goal is to optimize

$$\mathcal{P}_{\rm mse}(\tau):\begin{cases}\text{find} & \mathbf{W}_{\rm m},\mathbf{W}_{\rm f}\\ \text{s.t.} & \frac{\Re\{\mathbf{h}_{{\rm f},k}^{\dagger}\mathbf{w}_{{\rm f},k}\}}{\sqrt{\sum_{j\in\mathcal{K},j\neq k}|\mathbf{h}_{{\rm f},k}^{\dagger}\mathbf{w}_{{\rm f},j}|^2+\sum_{l\in\mathcal{L}}|\mathbf{h}_{{\rm m},k}^{\dagger}\mathbf{w}_{{\rm m},l}|^2+\sigma_{{\rm f},k}^2}}\geq\sqrt{\frac{1}{\tau\varepsilon_{{\rm f},k}}-1},\ \forall k\in\mathcal{K}\\ & \frac{\Re\{\mathbf{g}_{{\rm m},l}^{\dagger}\mathbf{w}_{{\rm m},l}\}}{\sqrt{\sum_{j\in\mathcal{L},j\neq l}|\mathbf{g}_{{\rm m},l}^{\dagger}\mathbf{w}_{{\rm m},j}|^2+\sum_{k\in\mathcal{K}}|\mathbf{g}_{{\rm f},l}^{\dagger}\mathbf{w}_{{\rm f},k}|^2+\sigma_{{\rm m},l}^2}}\geq\sqrt{\frac{1}{\varepsilon_{{\rm m},l}}-1},\quad\forall l\in\mathcal{L}\\ & \|\mathbf{W}_{\rm m}\|_{\rm F}^2\leq P_{\max,{\rm m}}\\ & \|\mathbf{W}_{\rm f}\|_{\rm F}^2\leq P_{\max,{\rm f}}.\end{cases}\tag{15}$$

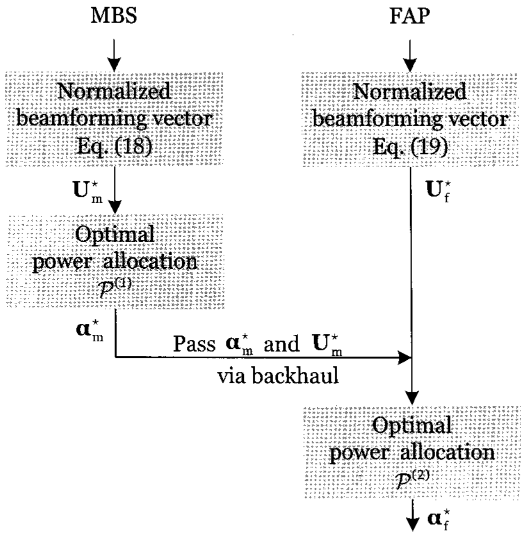

Fig. 3. Sequence of procedures for the semi-decentralized beamforming design.

the beamforming matrices $\mathbf{W}_{\mathrm{m}}$ and $\mathbf{W}_{\mathrm{f}}$ such that the aggregate network interference power is minimized while constraining the MSE of each user for the QoS guarantee. Specifically, we have the following problem formulation.

$$\mathcal{P}_{\mathrm{ip}}:\begin{cases}\min\limits_{\mathbf{W}_{\mathrm{m}},\mathbf{W}_{\mathrm{f}}} & \sum_{l\in\mathcal{L}}\sum_{k\in\mathcal{K}}\left(|\mathbf{g}_{\mathrm{f},l}^{\dagger}\mathbf{w}_{\mathrm{f},k}|^2+|\mathbf{h}_{\mathrm{m},k}^{\dagger}\mathbf{w}_{\mathrm{m},l}|^2\right)\\ \text{s.t.} & \mathsf{MSE}_{\mathrm{m},l}(\mathbf{W}_{\mathrm{m}},\mathbf{W}_{\mathrm{f}})\le\varepsilon_{\mathrm{m},l},\quad\forall l\in\mathcal{L}\\ & \mathsf{MSE}_{\mathrm{f},k}(\mathbf{W}_{\mathrm{m}},\mathbf{W}_{\mathrm{f}})\le\varepsilon_{\mathrm{f},k},\quad\forall k\in\mathcal{K}\\ & \|\mathbf{W}_{\mathrm{m}}\|_{\mathrm{F}}^2\le P_{\mathrm{max,m}}\\ & \|\mathbf{W}_{\mathrm{f}}\|_{\mathrm{F}}^2\le P_{\mathrm{max,f}}\end{cases}\tag{16}$$

where $\mathcal{P}_{\mathrm{ip}}$ in (16) can be cast as a convex optimization problem as (17), shown at the bottom of the page, which is also a SOCP.

IV. SEMI-DECENTRALIZED DESIGN

Although we can solve the optimization problems $\mathcal{P}_{\mathrm{tp}}$, $\mathcal{P}_{\mathrm{mse}}$, and $\mathcal{P}_{\mathrm{ip}}$ numerically in Section III, it is difficult to implement these centralized designs in practice since they require a backhaul equipment to obtain the global CSI as well as to compute the optimal beamforming matrices [25], [26]. Therefore, it is attractive to design practical semi-decentralized algorithms, where the MBS and FAP solve their own optimization problems *locally* with only minimal information exchange between the transmitters.[3]

For the semi-decentralized design, we first write $\mathbf{w}_{\mathrm{m},l}=\sqrt{\alpha_{\mathrm{m},l}}\mathbf{u}_{\mathrm{m},l}$ and $\mathbf{w}_{\mathrm{f},k}=\sqrt{\alpha_{\mathrm{f},k}}\mathbf{u}_{\mathrm{f},k}$, where $\alpha_{\mathrm{m},l}$ and $\alpha_{\mathrm{f},k}$ are the transmit powers allocated to MU_l and HU_k, respectively; and $\mathbf{u}_{\mathrm{m},l}\in\mathbb{C}^{N_{\mathrm{m}}\times 1}$ and $\mathbf{u}_{\mathrm{f},k}\in\mathbb{C}^{N_{\mathrm{f}}\times 1}$ are the normalized transmit beamforming vectors for MU_l and HU_k, respectively, i.e., $\|\mathbf{u}_{\mathrm{m},l}\|^2=\|\mathbf{u}_{\mathrm{f},k}\|^2=1$. Following [22]–[24], the normalized beamforming vectors for MU_l and HU_k are chosen to maximize their respective SLNRs as follows.

$$\begin{aligned}\mathbf{u}_{\mathrm{m},l}^{\star}&=\arg\max_{\|\mathbf{u}_{\mathrm{m},l}\|^2=1}\mathsf{SLNR}_{\mathrm{m},l}(\mathbf{W}_{\mathrm{m}})\\&=\boldsymbol{\lambda}_{\mathrm{gmax}}\left(\mathbf{G}_{\mathrm{m},l},\ \frac{\sigma_{\mathrm{m},l}^2}{N_{\mathrm{m}}}\mathbf{I}+\sum_{j\in\mathcal{L},j\neq l}\mathbf{G}_{\mathrm{m},j}+\sum_{k\in\mathcal{K}}\mathbf{H}_{\mathrm{m},k}\right)\end{aligned}\tag{18}$$

$$\begin{aligned}\mathbf{u}_{\mathrm{f},k}^{\star}&=\arg\max_{\|\mathbf{u}_{\mathrm{f},k}\|^2=1}\mathsf{SLNR}_{\mathrm{f},k}(\mathbf{W}_{\mathrm{f}})\\&=\boldsymbol{\lambda}_{\mathrm{gmax}}\left(\mathbf{H}_{\mathrm{f},k},\ \frac{\sigma_{\mathrm{f},k}^2}{N_{\mathrm{f}}}\mathbf{I}+\sum_{j\in\mathcal{K},j\neq k}\mathbf{H}_{\mathrm{f},j}+\sum_{l\in\mathcal{L}}\mathbf{G}_{\mathrm{f},l}\right)\end{aligned}\tag{19}$$

where $\mathbf{G}_{\mathrm{m},l}=\mathbf{g}_{\mathrm{m},l}\mathbf{g}_{\mathrm{m},l}^{\dagger}$, $\mathbf{G}_{\mathrm{f},l}=\mathbf{g}_{\mathrm{f},l}\mathbf{g}_{\mathrm{f},l}^{\dagger}$, $\mathbf{H}_{\mathrm{m},k}=\mathbf{h}_{\mathrm{m},k}\mathbf{h}_{\mathrm{m},k}^{\dagger}$, $\mathbf{H}_{\mathrm{f},k}=\mathbf{h}_{\mathrm{f},k}\mathbf{h}_{\mathrm{f},k}^{\dagger}$, and $\boldsymbol{\lambda}_{\mathrm{gmax}}(\mathbf{A},\mathbf{B})$ is the unit-norm dominant generalized eigenvector of a matrix pair $(\mathbf{A},\mathbf{B})$ corresponding to the largest generalized eigenvalue [22].[4] Next, we only need to determine the power allocations $\boldsymbol{\alpha}_{\mathrm{m}}=[\alpha_{\mathrm{m},1}\ \alpha_{\mathrm{m},2}\ \cdots\ \alpha_{\mathrm{m},l}]^T$ and $\boldsymbol{\alpha}_{\mathrm{f}}=[\alpha_{\mathrm{f},1}\ \alpha_{\mathrm{f},2}\ \cdots\ \alpha_{\mathrm{f},k}]^T$ for the MBS and FAP according to the specific optimization problem formulations in Section III. The sequence of procedures for the semi-decentralized beamforming design is depicted in Fig 3. For notational convenience, we denote $\mathbf{U}_{\mathrm{m}}^{\star}=[\mathbf{u}_{\mathrm{m},1}^{\star}\ \mathbf{u}_{\mathrm{m},2}^{\star}\ \cdots\ \mathbf{u}_{\mathrm{m},l}^{\star}]$ and $\mathbf{U}_{\mathrm{f}}^{\star}=[\mathbf{u}_{\mathrm{f},1}^{\star}\ \mathbf{u}_{\mathrm{f},2}^{\star}\ \cdots\ \mathbf{u}_{\mathrm{f},k}^{\star}]$.

A. Transmit Power Minimization Problem

Instead of jointly optimizing $\boldsymbol{\alpha}_{\mathrm{m}}$ and $\boldsymbol{\alpha}_{\mathrm{f}}$, we decouple $\mathcal{P}_{\mathrm{tp}}$ in (11) into two subproblems using $\mathbf{U}_{\mathrm{m}}^{\star}$ and $\mathbf{U}_{\mathrm{f}}^{\star}$ obtained by (18) and (19). The first subproblem is to solve the optimal power allocation problem for the MBS under the MSE constraint of each MU subject to maximum tolerable interference from the

[3] The centralized solutions can be leveraged to provide performance benchmarks for these semi-decentralized designs.

[4] For nonsingular $\mathbf{B}$, $\boldsymbol{\lambda}_{\mathrm{gmax}}(\mathbf{A},\mathbf{B})$ is equal to the unit-norm eigenvector corresponding to the largest eigenvalue of $\mathbf{B}^{-1}\mathbf{A}$.

$$\mathcal{P}_{\mathrm{ip}}:\begin{cases}\min\limits_{\mathbf{W}_{\mathrm{m}},\mathbf{W}_{\mathrm{f}}} & \sum_{l\in\mathcal{L}}\sum_{k\in\mathcal{K}}\left(|\mathbf{g}_{\mathrm{f},l}^{\dagger}\mathbf{w}_{\mathrm{f},k}|^2+|\mathbf{h}_{\mathrm{m},k}^{\dagger}\mathbf{w}_{\mathrm{m},l}|^2\right)\\ \text{s.t.} & \dfrac{\Re\mathfrak{e}\{\mathbf{g}_{\mathrm{m},l}^{\dagger}\mathbf{w}_{\mathrm{m},l}\}}{\sqrt{\sum_{j\in\mathcal{L},j\neq l}|\mathbf{g}_{\mathrm{m},l}^{\dagger}\mathbf{w}_{\mathrm{m},j}|^2+\sum_{k\in\mathcal{K}}|\mathbf{g}_{\mathrm{f},l}^{\dagger}\mathbf{w}_{\mathrm{f},k}|^2+\sigma_{\mathrm{m},l}^2}}\ge\sqrt{\dfrac{1}{\varepsilon_{\mathrm{m},l}}-1},\quad\forall l\in\mathcal{L}\\ & \dfrac{\Re\mathfrak{e}\{\mathbf{h}_{\mathrm{f},k}^{\dagger}\mathbf{w}_{\mathrm{f},k}\}}{\sqrt{\sum_{j\in\mathcal{L},j\neq k}|\mathbf{h}_{\mathrm{f},k}^{\dagger}\mathbf{w}_{\mathrm{f},j}|^2+\sum_{l\in\mathcal{L}}|\mathbf{h}_{\mathrm{m},k}^{\dagger}\mathbf{w}_{\mathrm{m},l}|^2+\sigma_{\mathrm{f},k}^2}}\ge\sqrt{\dfrac{1}{\varepsilon_{\mathrm{f},k}}-1},\quad\forall k\in\mathcal{K}\\ & \|\mathbf{W}_{\mathrm{m}}\|_{\mathrm{F}}^2\le P_{\mathrm{max,m}}\\ & \|\mathbf{W}_{\mathrm{f}}\|_{\mathrm{F}}^2\le P_{\mathrm{max,f}}\end{cases}\tag{17}$$

femtocell network. That is,

$$\mathcal{P}_{\rm tp}^{(1)}\left(\mathbf{U}_{\rm m}^\star\right):\begin{cases}\min\limits_{\boldsymbol{\alpha}_{\rm m}} & \mathbf{1}^T\boldsymbol{\alpha}_{\rm m}\\ \text{s.t.} & \frac{\alpha_{{\rm m},l}|\mathbf{g}_{{\rm m},l}^\dagger \mathbf{u}_{{\rm m},l}^\star|^2}{\sum_{j\in\mathcal{L},j\neq l}\alpha_{{\rm m},j}|\mathbf{g}_{{\rm m},l}^\dagger\mathbf{u}_{{\rm m},j}^\star|^2+P_{{\rm int},l}+\sigma_{{\rm m},l}^2}\\ & \geq\left(\frac{1}{\varepsilon_{{\rm m},l}}-1\right),\quad \forall l\in\mathcal{L}\end{cases}\tag{20}$$

where $P_{{\rm int},l}$ denotes the maximum tolerable level at MU_l for the femtocell network interference. Let $\boldsymbol{\alpha}_{\rm m}^\star$ be the optimal solution of $\mathcal{P}_{\rm tp}^{(1)}\left(\mathbf{U}_{\rm m}^\star\right)$. Then, following [35], the solution $\boldsymbol{\alpha}_{\rm m}^\star$ is given by

$$\boldsymbol{\alpha}_{\rm m}^\star=\left(\mathbf{I}-\mathbf{D}\left(\mathbf{U}_{\rm m}^\star,\boldsymbol{\varepsilon}_{\rm m}\right)\mathbf{F}\left(\mathbf{U}_{\rm m}^\star\right)\right)^{-1}\mathbf{v}\left(\mathbf{U}_{\rm m}^\star,\mathbf{P}_{\rm int}\right)\tag{21}$$

with $\boldsymbol{\varepsilon}_{\rm m}=\left[\varepsilon_{{\rm m},1}\ \varepsilon_{{\rm m},2}\ \cdots\ \varepsilon_{{\rm m},l}\right]^T$, $\mathbf{P}_{\rm int}=[P_{{\rm int},1}\ P_{{\rm int},2}\ \cdots\ P_{{\rm int},L}]^T$, $\mathbf{D}\left(\mathbf{U}_{\rm m}^\star,\boldsymbol{\varepsilon}_{\rm m}\right)\in\mathbb{R}_+^{L\times L}$, $\mathbf{v}(\mathbf{U}_{\rm m}^\star,\mathbf{P}_{\rm int})\in\mathbb{R}_+^{L\times 1}$, and $\mathbf{F}(\mathbf{U}_{\rm m}^\star)\in\mathbb{R}_+^{L\times L}$ whose (l,j)th entry is given by

$$F_{lj}(\mathbf{U}_{\rm m}^\star)=\begin{cases}0, & l=j\\ |\mathbf{g}_{{\rm m},l}^\dagger\mathbf{u}_{{\rm m},j}^\star|^2, & l\neq j\end{cases}\tag{22}$$

where

$$\mathbf{D}(\mathbf{U}_{\rm m}^\star,\boldsymbol{\varepsilon}_{\rm m})={\rm diag}\left(\frac{1/\varepsilon_{{\rm m},1}-1}{|\mathbf{g}_{{\rm m},1}^\dagger\mathbf{u}_{{\rm m},1}^\star|^2},\cdots,\frac{1/\varepsilon_{{\rm m},l}-1}{|\mathbf{g}_{{\rm m},l}^\dagger\mathbf{u}_{{\rm m},l}^\star|^2}\right),\tag{23}$$

$$\begin{aligned}&\mathbf{v}(\mathbf{U}_{\rm m}^\star,\mathbf{P}_{\rm int})\\&=\mathbf{D}(\mathbf{U}_{\rm m}^\star,\boldsymbol{\varepsilon}_{\rm m})\left[P_{{\rm int},1}+\sigma_{{\rm m},1}^2\cdots P_{{\rm int},L}+\sigma_{{\rm m},l}^2\right]^T.\end{aligned}\tag{24}$$

Using $\boldsymbol{\alpha}_{\rm m}^\star$ obtained in (21), we then solve the second subproblem given by (25), shown at the bottom of the page, which is a linear program (LP).

B. MSE Balancing Problem

Similar to subsection IV-A, we decouple $\mathcal{P}_{\rm mse}$ in (13) into two subproblems using $\mathbf{U}_{\rm m}^\star$ and $\mathbf{U}_{\rm f}^\star$ obtained in (18) and (19). The first subproblem to be solved is given by

$$\mathcal{P}_{\rm mse}^{(1)}(\mathbf{U}_{\rm m}^\star):\begin{cases}\min\limits_{\boldsymbol{\alpha}_{\rm m}} & \mathbf{1}^T\boldsymbol{\alpha}_{\rm m}\\ \text{s.t.} & \frac{\alpha_{{\rm m},l}|\mathbf{g}_{{\rm m},l}^\dagger \mathbf{u}_{{\rm m},l}^\star|^2}{\sum_{j\in\mathcal{L},j\neq l}\alpha_{{\rm m},j}|\mathbf{g}_{{\rm m},l}^\dagger\mathbf{u}_{{\rm m},j}^\star|^2+P_{{\rm int},l}+\sigma_{{\rm m},l}^2}\\ & \geq\left(\frac{1}{\varepsilon_{{\rm m},l}}-1\right),\quad \forall l\in\mathcal{L}\end{cases}\tag{26}$$

where $\boldsymbol{\alpha}_{\rm m}^\star$ is given in (21) and the second subproblem is given by

$$\begin{aligned}&\mathcal{P}_{\rm mse}^{(2)}(\mathbf{U}_{\rm m}^\star,\mathbf{U}_{\rm f}^\star,\boldsymbol{\alpha}_{\rm m}^\star):\\&\begin{cases}\min\limits_{\boldsymbol{\alpha}_{\rm f}} & \max_{k\in\mathcal{K}}\varepsilon_{{\rm f},k}^{-1}\mathsf{MSE}_{{\rm f},k}(\mathbf{U}_{\rm m}^\star,\mathbf{U}_{\rm f}^\star)\\ \text{s.t.} & \mathbf{1}^T\boldsymbol{\alpha}_{\rm f}\leq P_{\rm max,f}\\ & \sum_{k\in\mathcal{K}}\alpha_{{\rm f},k}|\mathbf{g}_{{\rm f},l}^\dagger\mathbf{u}_{{\rm f},k}^\star|^2\leq P_{{\rm int},l},\quad\forall l\in\mathcal{L}.\end{cases}\end{aligned}\tag{27}$$

Using a similar algorithm proposed to solve $\mathcal{P}_{\rm mse}$ in Section III, we can solve $\mathcal{P}_{\rm mse}^{(2)}(\mathbf{U}_{\rm m}^\star,\mathbf{U}_{\rm f}^\star,\boldsymbol{\alpha}_{\rm m}^\star)$ by rewriting (27) as follows.

$$\begin{aligned}&\mathcal{P}_{\rm mse}^{(2)}(\mathbf{U}_{\rm m}^\star,\mathbf{U}_{\rm f}^\star,\boldsymbol{\alpha}_{\rm m}^\star):\\&\begin{cases}\min\limits_{\boldsymbol{\alpha}_{\rm f},\tau} & \tau\\ \text{s.t.} & \mathsf{MSE}_{{\rm f},k}(\mathbf{U}_{\rm m}^\star,\mathbf{U}_{\rm f}^\star)\leq\tau\varepsilon_{{\rm f},k}\\ & \mathbf{1}^T\boldsymbol{\alpha}_{\rm f}\leq P_{\rm max,f}\\ & \sum_{k\in\mathcal{K}}\alpha_{{\rm f},k}|\mathbf{g}_{{\rm f},l}^\dagger\mathbf{u}_{{\rm f},k}^\star|^2\leq P_{{\rm int},l},\quad\forall l\in\mathcal{L}\end{cases}\end{aligned}\tag{28}$$

which can solved efficiently through a sequence of convex feasibility problem as (29), shown at the bottom of the page.

C. Network Interference Power Minimization Problem

We can decouple $\mathcal{P}_{\rm ip}$ in (16) into two subproblems as follows.

$$\begin{aligned}&\mathcal{P}_{\rm ip}^{(1)}(\mathbf{U}_{\rm m}^\star):\\&\begin{cases}\min\limits_{\boldsymbol{\alpha}_{\rm m}} & \sum_{l\in\mathcal{L}}\sum_{k\in\mathcal{K}}\alpha_{{\rm m},l}|\mathbf{h}_{{\rm m},k}^\dagger\mathbf{u}_{{\rm m},l}^\star|^2\\ \text{s.t.} & \frac{\alpha_{{\rm m},l}|\mathbf{g}_{{\rm m},l}^\dagger \mathbf{u}_{{\rm m},l}^\star|^2}{\sum_{j\in\mathcal{L},j\neq l}\alpha_{{\rm m},j}|\mathbf{g}_{{\rm m},l}^\dagger\mathbf{u}_{{\rm m},j}^\star|^2+P_{{\rm int},l}+\sigma_{{\rm m},l}^2}\\ & \geq\left(\frac{1}{\varepsilon_{{\rm m},l}}-1\right),\quad \forall l\in\mathcal{L}\\ & \mathbf{1}^T\boldsymbol{\alpha}_{\rm m}\leq P_{\rm max,m}\end{cases}\end{aligned}\tag{30}$$

$$\begin{aligned}&\mathcal{P}_{\rm ip}^{(2)}(\mathbf{U}_{\rm m}^\star,\mathbf{U}_{\rm f}^\star,\boldsymbol{\alpha}_{\rm m}^\star):\\&\begin{cases}\min\limits_{\boldsymbol{\alpha}_{\rm f}} & \sum_{l\in\mathcal{L}}\sum_{k\in\mathcal{K}}\alpha_{{\rm f},k}|\mathbf{g}_{{\rm m},l}^\dagger\mathbf{u}_{{\rm f},k}^\star|^2\\ \text{s.t.} & \frac{\alpha_{{\rm f},k}|\mathbf{h}_{{\rm f},k}^\dagger\mathbf{u}_{{\rm f},k}^\star|^2}{\sum_{j\in\mathcal{K},j\neq k}\alpha_{{\rm f},j}|\mathbf{h}_{{\rm f},k}^\dagger\mathbf{u}_{{\rm f},j}^\star|^2+\sum_{l\in\mathcal{L}}\alpha_{{\rm m},l}^\star|\mathbf{h}_{{\rm m},k}^\dagger\mathbf{u}_{{\rm m},l}^\star|^2+\sigma_{{\rm f},k}^2}\\ & \geq\left(\frac{1}{\varepsilon_{{\rm f},k}}-1\right),\quad\forall k\in\mathcal{K}\\ & \sum_{k\in\mathcal{K}}\alpha_{{\rm f},k}|\mathbf{g}_{{\rm f},l}^\dagger\mathbf{u}_{{\rm f},k}^\star|^2\leq P_{{\rm int},l},\quad\forall l\in\mathcal{L}\\ & \mathbf{1}^T\boldsymbol{\alpha}_{\rm f}\leq P_{\rm max,f}\end{cases}\end{aligned}\tag{31}$$

$$\mathcal{P}_{\rm tp}^{(2)}(\mathbf{U}_{\rm m}^\star,\mathbf{U}_{\rm f}^\star,\boldsymbol{\alpha}_{\rm m}^\star):\begin{cases}\min\limits_{\boldsymbol{\alpha}_{\rm f}} & \mathbf{1}^{\rm T}\boldsymbol{\alpha}_{\rm f}\\ \text{s.t.} & \frac{\alpha_{{\rm f},k}|\mathbf{h}_{{\rm f},k}^\dagger\mathbf{u}_{{\rm f},k}^\star|^2}{\sum_{j\in\mathcal{K},j\neq k}\alpha_{{\rm f},j}|\mathbf{h}_{{\rm f},k}^\dagger\mathbf{u}_{{\rm f},j}^\star|^2+\sum_{l\in\mathcal{L}}\alpha_{{\rm m},l}^\star|\mathbf{h}_{{\rm m},k}^\dagger\mathbf{u}_{{\rm m},l}^\star|^2+\sigma_{{\rm f},k}^2}\geq\left(\frac{1}{\varepsilon_{{\rm f},k}}-1\right),\quad\forall k\in\mathcal{K}\\ & \sum_{k\in\mathcal{K}}\alpha_{{\rm f},k}|\mathbf{g}_{{\rm f},l}^\dagger\mathbf{u}_{{\rm f},k}^\star|^2\leq P_{{\rm int},l},\quad\forall l\in\mathcal{L}\end{cases}\tag{25}$$

$$\mathcal{P}_{\rm mse}^{(2)}(\mathbf{U}_{\rm m}^\star,\mathbf{U}_{\rm f}^\star,\boldsymbol{\alpha}_{\rm m}^\star,\tau):\begin{cases}\text{find} & \boldsymbol{\alpha}_{\rm f}\\ \text{s.t.} & \frac{\alpha_{{\rm f},k}|\mathbf{h}_{{\rm f},k}^\dagger\mathbf{u}_{{\rm f},k}^\star|^2}{\sum_{j\in\mathcal{K},j\neq k}\alpha_{{\rm f},j}|\mathbf{h}_{{\rm f},k}^\dagger\mathbf{u}_{{\rm f},j}^\star|^2+\sum_{l\in\mathcal{L}}\alpha_{{\rm m},l}|\mathbf{h}_{{\rm m},k}^\dagger\mathbf{u}_{{\rm m},l}^\star|^2+\sigma_{{\rm f},k}^2}\geq\left(\frac{1}{\tau\varepsilon_{{\rm f},k}}-1\right),\quad\forall k\in\mathcal{K}\\ & \mathbf{1}^T\boldsymbol{\alpha}_{\rm f}\leq P_{\rm max,f}\\ & \sum_{k\in\mathcal{K}}\alpha_{{\rm f},k}|\mathbf{g}_{{\rm f},l}^\dagger\mathbf{u}_{{\rm f},k}^\star|^2\leq P_{{\rm int},l},\quad\forall l\in\mathcal{L}.\end{cases}\tag{29}$$

where $\boldsymbol{\alpha}_{\rm m}^\star$ is given in (21) and $\mathcal{P}_{\rm ip}^{(2)}(\mathbf{U}_{\rm m}^\star, \mathbf{U}_{\rm f}^\star, \boldsymbol{\alpha}_{\rm m}^\star)$ is simply an LP.

Remark 4: The main advantage of the semi-decentralized designs is that the amount of CSI required to solve each of the subproblems is smaller than the centralized designs in Section III. Moreover, each subproblem can be solved at each transmitter only requiring the availability of backhaul signaling to pass $\boldsymbol{\alpha}_{\rm m}^\star$ and $\mathbf{U}_{\rm m}^\star$ from the MBS to the FAP.

V. ROBUST DESIGN WITH IMPERFECT CSI

In Sections III and IV, the perfect CSI is assumed to be available at the transmitters, which may not always be practical due to the inherent time-varying nature of wireless propagation channels and the mobility of users. As such, we further consider robust beamforming and power control design in the case of erroneous CSI using the worst case design [28]– [27]. Specifically, we treat uncertainty by assuming that CSI is a deterministic variable within a bounded set of possible values, i.e., estimated channel vectors are known with estimation errors lying in some bounded sets of known size. In this section, we only consider the transmit power minimization problem with imperfect CSI for both the centralized and semi-decentralized cases, and other optimization problems can be similarly extended to the case of imperfect CSI.

In the following, we model the channel covariance uncertainty in (18) and (19) as follows.

$$\mathbf{G}_{{\rm m},l} = \widehat{\mathbf{G}}_{{\rm m},l} + \boldsymbol{\Delta}_{{\rm m},l} \tag{32}$$

$$\mathbf{G}_{{\rm f},l} = \widehat{\mathbf{G}}_{{\rm f},l} + \boldsymbol{\Delta}_{{\rm f},l} \tag{33}$$

$$\mathbf{H}_{{\rm m},k} = \widehat{\mathbf{H}}_{{\rm m},k} + \boldsymbol{\Theta}_{{\rm m},k} \tag{34}$$

$$\mathbf{H}_{{\rm f},k} = \widehat{\mathbf{H}}_{{\rm f},k} + \boldsymbol{\Theta}_{{\rm f},k} \tag{35}$$

where $\widehat{\mathbf{G}}_{{\rm m},l}$ and $\widehat{\mathbf{H}}_{{\rm m},k}$ are the estimated channel covariance matrices from the MBS to MU_l and HU_k, respectively; $\widehat{\mathbf{G}}_{{\rm f},l}$ and $\widehat{\mathbf{H}}_{{\rm f},k}$ are the estimated channel covariance matrices from the FAP to MU_l and HU_k, respectively; and $\boldsymbol{\Delta}_{{\rm m},l}$, $\boldsymbol{\Delta}_{{\rm f},l}$, $\boldsymbol{\Theta}_{{\rm m},k}$, and $\boldsymbol{\Theta}_{{\rm f},k}$ denote the corresponding uncertainties with bounded Frobenius norms given by $\|\boldsymbol{\Delta}_{{\rm m},l}\|_{\rm F} \le \delta_{{\rm m},l}$, $\|\boldsymbol{\Delta}_{{\rm f},l}\|_{\rm F} \le \delta_{{\rm f},l}$, $\|\boldsymbol{\Theta}_{{\rm m},k}\|_{\rm F} \le \eta_{{\rm m},k}$, and $\|\boldsymbol{\Theta}_{{\rm f},k}\|_{\rm F} \le \eta_{{\rm f},k}$.

A. Centralized Design

The robust version of (11) can then be formulated as (36). Using the worst-case approach, we can approximate the robust formulation (36) as (37), shown at the bottom of the page [36]. By letting $\mathbf{W}_{{\rm m},l} = \mathbf{w}_{{\rm m},l}\mathbf{w}_{{\rm m},l}^\dagger$ and $\mathbf{W}_{{\rm f},k} = \mathbf{w}_{{\rm f},k}\mathbf{w}_{{\rm f},k}^\dagger$, we can transform (37) into a semi-definite program (SDP) by ignoring the rank-1 constraint as (38), shown at the bottom of the page, which can solved efficiently using standard convex optimization algorithms.

B. Semi-Decentralized Design

Using the channel covariance uncertainty defined in (32)–(35), the robust normalized beamforming vectors for MU_l and HU_k are chosen to maximize their respective robust SLNRs as follows.

$$\mathbf{u}_{{\rm m},l}^{\rm rob} = \arg \max_{\|\mathbf{u}_{{\rm m},l}\|^2=1} \min_{\substack{\|\boldsymbol{\Delta}_{{\rm m},l}\|_{\rm F}\le\delta_{{\rm m},l} \\ \|\boldsymbol{\Theta}_{{\rm m},k}\|_{\rm F}\le\eta_{{\rm m},k}}} \mathsf{SLNR}_{{\rm m},l}(\mathbf{W}_{\rm m}) \tag{39}$$

$$\mathbf{u}_{{\rm f},k}^{\rm rob} = \arg \max_{\|\mathbf{u}_{{\rm f},k}\|^2=1} \min_{\substack{\|\boldsymbol{\Delta}_{{\rm f},l}\|_{\rm F}\le\delta_{{\rm f},l} \\ \|\boldsymbol{\Theta}_{{\rm f},k}\|_{\rm F}\le\eta_{{\rm f},k}}} \mathsf{SLNR}_{{\rm f},k}(\mathbf{W}_{\rm f}). \tag{40}$$

Following the worst-case approach in [36], we can approximate the robust beamforming vectors in (39) and (40) as (41) and (42). Using (41) and letting $\mathbf{U}_{\rm m}^{\rm rob} = [\mathbf{u}_{{\rm m},1}^{\rm rob}\ \mathbf{u}_{{\rm m},2}^{\rm rob}\ \cdots\ \mathbf{u}_{{\rm m},l}^{\rm rob}]$, the

$$\begin{aligned} \min_{\mathbf{W}_{\rm m},\mathbf{W}_{\rm f}} \quad & \|\mathbf{W}_{\rm m}\|_{\rm F}^2 + \|\mathbf{W}_{\rm f}\|_{\rm F}^2 \\ \text{s.t.} \quad & \min_{\substack{\|\boldsymbol{\Delta}_{{\rm m},l}\|_{\rm F}\le\delta_{{\rm m},l} \\ \|\boldsymbol{\Delta}_{{\rm f},l}\|_{\rm F}\le\delta_{{\rm f},l}}} \frac{\mathbf{w}_{{\rm m},l}^\dagger \mathbf{G}_{{\rm m},l}\mathbf{w}_{{\rm m},l}}{\sum_{j\in\mathcal{L},j\ne l}\mathbf{w}_{{\rm m},j}^\dagger\mathbf{G}_{{\rm m},l}\mathbf{w}_{{\rm m},j} + \sum_{k\in\mathcal{K}}\mathbf{w}_{{\rm f},k}^\dagger\mathbf{G}_{{\rm f},l}\mathbf{w}_{{\rm f},k} + \sigma_{{\rm m},l}^2} \ge \left(\frac{1}{\varepsilon_{{\rm m},l}} - 1\right), \quad \forall l\in\mathcal{L} \\ & \min_{\substack{\|\boldsymbol{\Theta}_{{\rm m},k}\|_{\rm F}\le\eta_{{\rm m},k} \\ \|\boldsymbol{\Theta}_{{\rm f},k}\|_{\rm F}\le\eta_{{\rm f},k}}} \frac{\mathbf{w}_{{\rm f},k}^\dagger \mathbf{H}_{{\rm f},k}\mathbf{w}_{{\rm f},k}}{\sum_{j\in\mathcal{K},j\ne k}\mathbf{w}_{{\rm f},j}^\dagger\mathbf{H}_{{\rm f},k}\mathbf{w}_{{\rm f},j} + \sum_{l\in\mathcal{L}}\mathbf{w}_{{\rm m},l}^\dagger\mathbf{H}_{{\rm m},k}\mathbf{w}_{{\rm m},l} + \sigma_{{\rm f},k}^2} \ge \left(\frac{1}{\varepsilon_{{\rm f},k}} - 1\right), \quad \forall k\in\mathcal{K}. \end{aligned} \tag{36}$$

$$\begin{aligned} \min_{\mathbf{W}_{\rm m},\mathbf{W}_{\rm f}} \quad & \|\mathbf{W}_{\rm m}\|_{\rm F}^2 + \|\mathbf{W}_{\rm f}\|_{\rm F}^2 \\ \text{s.t.} \quad & \frac{\mathbf{w}_{{\rm m},l}^\dagger(\widehat{\mathbf{G}}_{{\rm m},l} - \delta_{{\rm m},l}\mathbf{I})\mathbf{w}_{{\rm m},l}}{\sum_{j\in\mathcal{L},j\ne l}\mathbf{w}_{{\rm m},j}^\dagger(\widehat{\mathbf{G}}_{{\rm m},l}+\delta_{{\rm m},l}\mathbf{I})\mathbf{w}_{{\rm m},j} + \sum_{k\in\mathcal{K}}\mathbf{w}_{{\rm f},k}^\dagger(\widehat{\mathbf{G}}_{{\rm f},l}+\delta_{{\rm f},l}\mathbf{I})\mathbf{w}_{{\rm f},k} + \sigma_{{\rm m},l}^2} \ge \left(\frac{1}{\varepsilon_{{\rm m},l}} - 1\right), \quad \forall l\in\mathcal{L} \\ & \frac{\mathbf{w}_{{\rm f},k}^\dagger(\widehat{\mathbf{H}}_{{\rm f},k} - \eta_{{\rm f},k}\mathbf{I})\mathbf{w}_{{\rm f},k}}{\sum_{j\in\mathcal{K},j\ne k}\mathbf{w}_{{\rm f},j}^\dagger(\widehat{\mathbf{H}}_{{\rm f},k}+\eta_{{\rm f},k}\mathbf{I})\mathbf{w}_{{\rm f},j} + \sum_{l\in\mathcal{L}}\mathbf{w}_{{\rm m},l}^\dagger(\widehat{\mathbf{H}}_{{\rm m},k}+\eta_{{\rm m},k}\mathbf{I})\mathbf{w}_{{\rm m},l} + \sigma_{{\rm f},k}^2} \ge \left(\frac{1}{\varepsilon_{{\rm f},k}} - 1\right), \quad \forall k\in\mathcal{K}. \end{aligned} \tag{37}$$

$$\mathcal{P}_{\text{robust-tp}} : \begin{cases} \min\limits_{\mathbf{W}_{\rm m},\mathbf{W}_{\rm f}} & \sum_{l\in\mathcal{L}}\operatorname{tr}(\mathbf{W}_{{\rm m},l}) + \sum_{k\in\mathcal{K}}\operatorname{tr}(\mathbf{W}_{{\rm f},k}) \\ \text{s.t.} & \dfrac{\operatorname{tr}(\widehat{\mathbf{G}}_{{\rm m},l}\mathbf{W}_{{\rm m},l} - \delta_{{\rm m},l}\mathbf{W}_{{\rm m},l})}{\sum_{j\in\mathcal{L},j\ne l}\operatorname{tr}(\widehat{\mathbf{G}}_{{\rm m},l}\mathbf{W}_{{\rm m},j}+\delta_{{\rm m},l}\mathbf{W}_{{\rm m},j}) + \sum_{k\in\mathcal{K}}\operatorname{tr}(\widehat{\mathbf{G}}_{{\rm f},l}\mathbf{W}_{{\rm f},k}+\delta_{{\rm f},l}\mathbf{W}_{{\rm f},k}) + \sigma_{{\rm m},l}^2} \ge \left(\frac{1}{\varepsilon_{{\rm m},l}} - 1\right), \quad \forall l\in\mathcal{L} \\ & \dfrac{\operatorname{tr}(\widehat{\mathbf{H}}_{{\rm f},k}\mathbf{W}_{{\rm f},k} - \eta_{{\rm f},k}\mathbf{W}_{{\rm f},k})}{\sum_{j\in\mathcal{K},j\ne k}\operatorname{tr}(\widehat{\mathbf{H}}_{{\rm f},k}\mathbf{W}_{{\rm f},j}+\eta_{{\rm f},k}\mathbf{W}_{{\rm f},j}) + \sum_{l\in\mathcal{L}}\operatorname{tr}(\widehat{\mathbf{H}}_{{\rm m},k}\mathbf{W}_{{\rm m},l}+\eta_{{\rm m},k}\mathbf{W}_{{\rm m},l}) + \sigma_{{\rm f},k}^2} \ge \left(\frac{1}{\varepsilon_{{\rm f},k}} - 1\right), \quad \forall k\in\mathcal{K}. \end{cases} \tag{38}$$

first robust subproblem can be formulated as (43), which can be further approximated as (44), shown at the bottom of the page. Let $\boldsymbol{\alpha}_{\rm m}^{\rm rob}$ be the optimal solution of $\mathcal{P}_{\rm tp}^{(1)}(\mathbf{U}_{\rm m}^{\rm rob})$. Then, we have

$$\boldsymbol{\alpha}_{\rm m}^{\rm rob} = \left(\mathbf{I} - \mathbf{D}\left(\mathbf{U}_{\rm m}^{\rm rob}, \boldsymbol{\varepsilon}_{\rm m}\right)\mathbf{F}\left(\mathbf{U}_{\rm m}^{\rm rob}\right)\right)^{-1}\mathbf{v}\left(\mathbf{U}_{\rm m}^{\rm rob}, \mathbf{P}_{\rm int}\right) \quad (45)$$

with $\mathbf{D}(\mathbf{U}_{\rm m}^{\rm rob}, \boldsymbol{\varepsilon}_{\rm m}) \in \mathbb{R}_{+}^{L\times L}$, $\mathbf{v}(\mathbf{U}_{\rm m}^{\rm rob}, \mathbf{P}_{\rm int}) \in \mathbb{R}_{+}^{L\times 1}$, and $\mathbf{F}(\mathbf{U}_{\rm m}^{\rm rob}) \in \mathbb{R}_{+}^{L\times L}$ whose (l,j)th entry is given by

$$F_{lj}(\mathbf{U}_{\rm m}^{\rm rob}) = \begin{cases} 0, & l = j \\ \mathbf{u}_{{\rm m},j}^{{\rm rob}\dagger}\left(\widehat{\mathbf{G}}_{{\rm m},l} + \delta_{{\rm m},l}\mathbf{I}\right)\mathbf{u}_{{\rm m},j}^{\rm rob}, & l \neq j \end{cases} \quad (46)$$

where

$$\mathbf{D}\left(\mathbf{U}_{\rm m}^{\rm rob}, \varepsilon_{\rm m}\right) = \mathrm{diag}\left(\frac{1/\varepsilon_{{\rm m},1} - 1}{\mathbf{u}_{{\rm m},1}^{{\rm rob}\dagger}\left(\widehat{\mathbf{G}}_{{\rm m},1} - \delta_{{\rm m},1}\mathbf{I}\right)\mathbf{u}_{{\rm m},1}^{\rm rob}}, \cdots, \frac{1/\varepsilon_{{\rm m},l} - 1}{\mathbf{u}_{{\rm m},l}^{{\rm rob}\dagger}\left(\widehat{\mathbf{G}}_{{\rm m},l} - \delta_{{\rm m},l}\mathbf{I}\right)\mathbf{u}_{{\rm m},l}^{\rm rob}}\right) \quad (47)$$

and

$$\mathbf{v}(\mathbf{U}_{\rm m}^{\rm rob}, \mathbf{P}_{\rm int}) = \mathbf{D}(\mathbf{U}_{\rm m}^{\rm rob}, \boldsymbol{\varepsilon}_{\rm m})\left[P_{{\rm int},1} + \sigma_{{\rm m},1}^2, \cdots, P_{{\rm int},L} + \sigma_{{\rm m},l}^2\right]^T. \quad (48)$$

Using $\boldsymbol{\alpha}_{\rm m}^{\rm rob}$ obtained in (45), we then solve the second subproblem given by (49), which can be approximated as an LP as (50), shown at the bottom of the next page.

VI. NUMERICAL RESULTS

In this section, we present numerical results to illustrate the performance of our proposed algorithms. The FAP is located at the origin of two-dimensional space and the MBS is at 30-meter distant from the FAP, i.e., the FAP and MBS are fixed at $(x,y) = (0,0)$ and $(30,0)$, respectively. Furthermore, we assume that the MUs are located at the same position $(d,0)$ while the HUs are at $(3,0)$, for simplicity. Using a path-loss exponent model, we can relate the x-axis value d of MUs to the amount of femtocell network interference at the MUs. We consider Rayleigh fading such that

- The outdoor link path-loss exponent is set to 4, i.e., the entries of $\mathbf{g}_{{\rm m},l}^{\dagger}$ is circularly symmetric complex Gaussian $\mathcal{CN}\left(0, 1/|30-d|^4\right)$;
- the indoor link path-loss exponent is set to 3, i.e., the entries of $\mathbf{h}_{{\rm f},k}^{\dagger}$ is $\mathcal{CN}\left(0, 1/3^3\right)$; and
- the outdoor-to-indoor or indoor-to-outdoor link path-loss exponent is set to 3.7, i.e., the entries of $\mathbf{g}_{{\rm f},l}^{\dagger}$ and $\mathbf{h}_{{\rm m},k}^{\dagger}$ are $\mathcal{CN}\left(0, 1/|d|^{3.7}\right)$ and $\mathcal{CN}\left(0, 1/27^{3.7}\right)$, respectively.

In addition, we set $N_{\rm m} = N_{\rm f} = 4$, $\sigma_{{\rm m},l}^2 = \sigma_{{\rm f},k}^2 = 1$, and $L = K = 2$ (except for the MSE balancing problem). When the MUs and HUs have the same MSE QoS constraints (i.e., equal QoS priority), we denote those values by $\varepsilon_{\rm m}$ and $\varepsilon_{\rm f}$, respectively, i.e., $\varepsilon_{\rm m} = \varepsilon_{{\rm m},1} = \cdots = \varepsilon_{{\rm m},L}$ and $\varepsilon_{\rm f} = \varepsilon_{{\rm f},1} = \cdots = \varepsilon_{{\rm f},K}$.

We first consider the total transmit power minimization problem when the MSE QoS constraints are fixed while the location of MUs vary. In semi-decentralized design, we need to specify the maximum tolerable interference level $\mathbf{P}_{\rm int}$ for the MUs, which allows us to decouple each optimization problem into two subproblems as described in subsection IV-A. In the examples, we set the same tolerable level for all MUs as $P_{\rm int} = P_{{\rm int},1} = \cdots = P_{{\rm int},L}$. Fig. 4 shows the total transmit power for the centralized design in subsection III-A and the semi-decentralized design in subsection IV-A as a function of the x-axis value d (meters) of MUs when $\varepsilon = \varepsilon_{\rm m} = \varepsilon_{\rm f} = 0.6$, 0.8, and $P_{\rm int} = 3$ dB for the semi-decentralized design. We can observe that the total transmit power decreases with the MSE constraint ε and the distance d. As ε increases, the users' QoS becomes less strict, while the femtocell interference becomes less severe due to larger path losses, as d increases. The semi-decentralized processing enables us to design the power minimization algorithm requiring no global CSI at the price of a larger total transmit power to satisfy the MSE QoS at each user.

$$\mathbf{u}_{{\rm m},l}^{\rm rob} = \lambda_{\rm gmax}\left(\widehat{\mathbf{G}}_{{\rm m},l} - \delta_{{\rm m},l}\mathbf{I}, \frac{\sigma_{{\rm m},l}^2}{N_{\rm m}}\mathbf{I} + \sum_{j\in\mathcal{L}, j\neq l}\left(\widehat{\mathbf{G}}_{{\rm m},j} + \delta_{{\rm m},j}\mathbf{I}\right) + \sum_{k\in\mathcal{K}}\left(\widehat{\mathbf{H}}_{{\rm m},k} + \eta_{{\rm m},k}\mathbf{I}\right)\right) \quad (41)$$

$$\mathbf{u}_{{\rm f},k}^{\rm rob} = \lambda_{\rm gmax}\left(\widehat{\mathbf{H}}_{{\rm f},k} - \eta_{{\rm f},k}\mathbf{I}, \frac{\sigma_{{\rm f},k}^2}{N_{\rm f}}\mathbf{I} + \sum_{j\in\mathcal{K}, j\neq k}\left(\widehat{\mathbf{H}}_{{\rm f},j} + \eta_{{\rm f},j}\mathbf{I}\right) + \sum_{l\in\mathcal{L}}\left(\widehat{\mathbf{G}}_{{\rm f},l} + \delta_{{\rm f},l}\mathbf{I}\right)\right). \quad (42)$$

$$\mathcal{P}_{\rm tp}^{(1)}(\mathbf{U}_{\rm m}^{\rm rob}) : \begin{cases} \min\limits_{\boldsymbol{\alpha}_{\rm m}} & \mathbf{1}^T\boldsymbol{\alpha}_{\rm m} \\ \text{s.t.} & \min\limits_{\|\boldsymbol{\Delta}_{{\rm m},l}\|_F \le \delta_{{\rm m},l}} \dfrac{\alpha_{{\rm m},l}\mathbf{u}_{{\rm m},l}^{{\rm rob}\dagger}\mathbf{G}_{{\rm m},l}\mathbf{u}_{{\rm m},l}^{\rm rob}}{\sum_{j\in\mathcal{L}, j\neq l}\alpha_{{\rm m},j}\mathbf{u}_{{\rm m},j}^{{\rm rob}\dagger}\mathbf{G}_{{\rm m},l}\mathbf{u}_{{\rm m},j}^{\rm rob} + P_{{\rm int},l} + \sigma_{{\rm m},l}^2} \ge \left(\dfrac{1}{\varepsilon_{{\rm m},l}} - 1\right), \quad \forall l \in \mathcal{L} \end{cases} \quad (43)$$

$$\mathcal{P}_{\rm tp}^{(1)}(\mathbf{U}_{\rm m}^{\rm rob}) : \begin{cases} \min\limits_{\boldsymbol{\alpha}_{\rm m}} & \mathbf{1}^T\boldsymbol{\alpha}_{\rm m} \\ \text{s.t.} & \dfrac{\alpha_{{\rm m},l}\mathbf{u}_{{\rm m},l}^{{\rm rob}\dagger}\left(\widehat{\mathbf{G}}_{{\rm m},l} - \delta_{{\rm m},l}\mathbf{I}\right)\mathbf{u}_{{\rm m},l}^{\rm rob}}{\sum_{j\in\mathcal{L}, j\neq l}\alpha_{{\rm m},j}\mathbf{u}_{{\rm m},j}^{{\rm rob}\dagger}\left(\widehat{\mathbf{G}}_{{\rm m},l} + \delta_{{\rm m},l}\mathbf{I}\right)\mathbf{u}_{{\rm m},j}^{\rm rob} + P_{{\rm int},l} + \sigma_{{\rm m},l}^2} \ge \left(\frac{1}{\varepsilon_{{\rm m},l}} - 1\right), \quad \forall l \in \mathcal{L}. \end{cases} \quad (44)$$

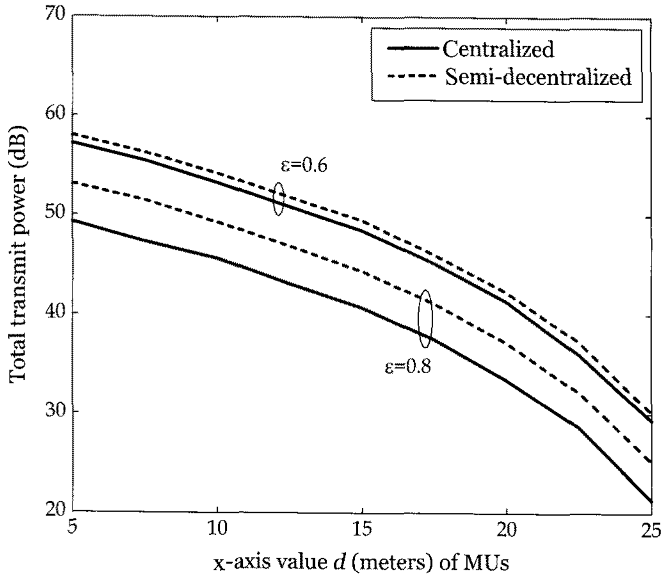

Fig. 4. Total transmit power for the centralized and the semi-decentralized designs as a function of the x-axis value d (meters) of MUs. $\varepsilon = \varepsilon_{\mathrm{m}} = \varepsilon_{\mathrm{f}} = 0.6$ and 0.8; and $P_{\mathrm{int}} = 3$ dB for the semi-decentralized design.

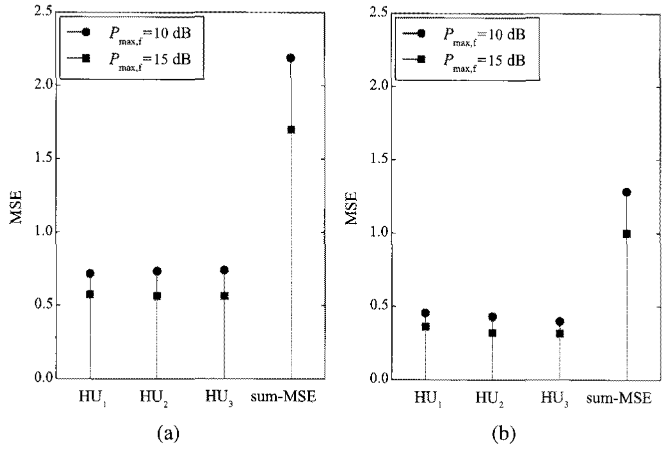

Fig. 5. MSE and sum-MSE of HUs for the centralized MSE balancing design $\mathcal{P}_{\mathrm{mse}}$. $d = 15$ meters, $L = 2$, $K = 3$, $\varepsilon_{\mathrm{m}} = 0.6$, $P_{\mathrm{max,m}} = 40$ dB, and $P_{\mathrm{max,f}} = 10$ dB and 15 dB for two cases: (a) Equal HU QoS priority ($\varepsilon_{\mathrm{f},1} = \varepsilon_{\mathrm{f},2} = \varepsilon_{\mathrm{f},3} = 0.6$) and (b) unequal HU QoS priority ($\varepsilon_{\mathrm{f},1} = 0.6$, $\varepsilon_{\mathrm{f},2} = 0.7$, $\varepsilon_{\mathrm{f},3} = 0.8$).

Fig. 5 shows the MSE and sum-MSE of HUs for the centralized MSE balancing design in subsection III-B when $L = 2$, $K = 3$, $\varepsilon_{\mathrm{m}} = 0.6$, $d = 15$ meters, $P_{\mathrm{max,m}} = 40$ dB, and $P_{\mathrm{max,f}} = 10$ dB and 15 dB for two cases: (a) Equal HU QoS priority ($\varepsilon_{\mathrm{f},1} = \varepsilon_{\mathrm{f},2} = \varepsilon_{\mathrm{f},3} = 0.6$) and (b) unequal HU QoS priority ($\varepsilon_{\mathrm{f},1} = 0.6$, $\varepsilon_{\mathrm{f},2} = 0.7$, $\varepsilon_{\mathrm{f},3} = 0.8$). We can see that the MSE is *nearly* balanced among the HUs for both equal and unequal HU QoS cases. Moreover, with a larger available power at each transmitter, we can reduce each HU MSE and hence the overall sum-MSE, showing the effectiveness of power allocation in improving the system QoS. Fig. 6 shows the MSE and sum-MSE of HUs for the semi-decentralized MSE balancing design in subsection IV-B when $L = 2$, $K = 3$, $\varepsilon_{\mathrm{m}} = 0.6$, $d = 15$ meters, $P_{\mathrm{int}} = 3$ dB, and $P_{\mathrm{max,m}} = 40$ dB, $P_{\mathrm{max,f}} = 10$ dB and 15 dB for two QoS priority cases as in Fig. 5. Similar to the centralized design, we can again observe the nearly-balanced MSE among the HUs for both cases. This reveals the semi-decentralized MSE balancing to be feasible at the cost of a larger HU MSE.

Fig. 7 shows the network interference power for the centralized design in subsection III-C and the semi-decentralized design in subsection IV-C as a function of the x-axis value d (meters) of MUs when $\varepsilon = \varepsilon_{\mathrm{m}} = \varepsilon_{\mathrm{f}} = 0.6$ and 0.8, $P_{\mathrm{max,m}} = 60$ dB, $P_{\mathrm{max,f}} = 20$ dB, and $P_{\mathrm{int}} = 3$ dB. We can again see that the network interference power decreases with the MSE constraint. The less strict user QoS reduces the required transmission power at each transmitter, which in turn decreases the network interference power. We can also see that as d increases, the network interference power decreases, which is due to the fact that larger path losses reduce the femtocell network interference at the MUs. Similarly, we can observe that the network interference minimization is still feasible in the semi-decentralized framework at the cost of a larger interference power.

For the robust design example with imperfect CSI, we set simply the Frobenius-norm bounds of uncertainty as $\rho = \delta_{\mathrm{f},l} = \eta_{\mathrm{m},k}$ (cross-tier links) and $\delta_{\mathrm{m},l} = \eta_{\mathrm{f},k} = 0$ for all $l \in \mathcal{L}$, $k \in \mathcal{K}$. Fig. 8 shows the total transmit power for the robust centralized

$$
\begin{aligned}
\min_{\boldsymbol{\alpha}_{\mathrm{f}}} \quad & \mathbf{1}^T \boldsymbol{\alpha}_{\mathrm{f}} \\
\text{s.t.} \quad & \min_{\substack{\|\boldsymbol{\Theta}_{\mathrm{m},k}\|_F \le \eta_{\mathrm{m},k} \\ \|\boldsymbol{\Theta}_{\mathrm{f},k}\|_F \le \eta_{\mathrm{f},k}}} \frac{\alpha_{\mathrm{f},k} \mathbf{u}_{\mathrm{f},k}^{\mathrm{rob}\dagger} \mathbf{H}_{\mathrm{f},k} \mathbf{u}_{\mathrm{f},k}^{\mathrm{rob}}}{\sum_{j \in \mathcal{K}, j \neq k} \alpha_{\mathrm{f},j} \mathbf{u}_{\mathrm{f},j}^{\mathrm{rob}\dagger} \mathbf{H}_{\mathrm{f},k} \mathbf{u}_{\mathrm{f},j}^{\mathrm{rob}} + \sum_{l \in \mathcal{L}} \alpha_{\mathrm{m},l}^{\mathrm{rob}} \mathbf{u}_{\mathrm{m},l}^{\mathrm{rob}\dagger} \mathbf{H}_{\mathrm{m},k} \mathbf{u}_{\mathrm{m},l}^{\mathrm{rob}} + \sigma_{\mathrm{f},k}^2} \ge \left(\frac{1}{\varepsilon_{\mathrm{f},k}} - 1 \right), \quad \forall k \in \mathcal{K} \\
& \min_{\|\boldsymbol{\Delta}_{\mathrm{f},l}\|_F \le \delta_{\mathrm{f},l}} \sum_{k \in \mathcal{K}} \alpha_{\mathrm{f},k} \mathbf{u}_{\mathrm{f},k}^{\mathrm{rob}\dagger} \mathbf{G}_{\mathrm{f},l} \mathbf{u}_{\mathrm{f},k}^{\mathrm{rob}} \le P_{\mathrm{int},l}, \quad \forall l \in \mathcal{L}
\end{aligned} \tag{49}
$$

$$
\mathcal{P}_{\mathrm{robust-tp}}^{(2)}(\mathbf{U}_{\mathrm{p}}^{\mathrm{rob}}, \mathbf{U}_{\mathrm{s}}^{\mathrm{rob}}, \boldsymbol{\alpha}_{\mathrm{p}}^{\mathrm{rob}}) : \left\{ \begin{aligned}
\min_{\boldsymbol{\alpha}_{\mathrm{f}}} \quad & \mathbf{1}^T \boldsymbol{\alpha}_{\mathrm{f}} \\
\text{s.t.} \quad & \frac{\alpha_{\mathrm{f},k} \mathbf{u}_{\mathrm{f},k}^{\mathrm{rob}\dagger} (\widehat{\mathbf{H}}_{\mathrm{f},k} - \eta_{\mathrm{f},k} \mathbf{I}) \mathbf{u}_{\mathrm{f},k}^{\mathrm{rob}}}{\sum_{j \in \mathcal{K}, j \neq k} \alpha_{\mathrm{f},j} \mathbf{u}_{\mathrm{f},j}^{\mathrm{rob}\dagger} (\widehat{\mathbf{H}}_{\mathrm{f},k} + \eta_{\mathrm{f},k} \mathbf{I}) \mathbf{u}_{\mathrm{f},j}^{\mathrm{rob}} + \sum_{l \in \mathcal{L}} \alpha_{\mathrm{m},l}^{\mathrm{rob}} \mathbf{u}_{\mathrm{m},l}^{\mathrm{rob}\dagger} (\widehat{\mathbf{H}}_{\mathrm{m},k} + \eta_{\mathrm{m},k} \mathbf{I}) \mathbf{u}_{\mathrm{m},l}^{\mathrm{rob}} + \sigma_{\mathrm{f},k}^2} \\
& \ge \left(\frac{1}{\varepsilon_{\mathrm{f},k}} - 1 \right), \quad \forall k \in \mathcal{K} \\
& \sum_{k \in \mathcal{K}} \alpha_{\mathrm{f},k} \mathbf{u}_{\mathrm{f},k}^{\mathrm{rob}\dagger} \left(\widehat{\mathbf{G}}_{\mathrm{f},l} + \delta_{\mathrm{f},l} \mathbf{I} \right) \mathbf{u}_{\mathrm{f},k}^{\mathrm{rob}} \le P_{\mathrm{int},l}, \quad \forall l \in \mathcal{L}.
\end{aligned} \right. \tag{50}
$$

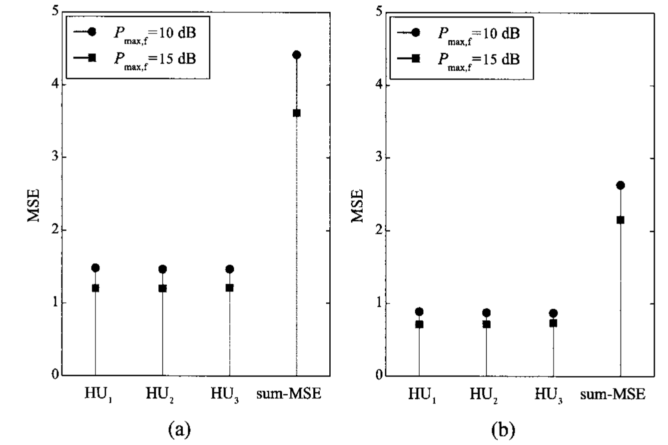

Fig. 6. MSE and sum-MSE of HUs for the decentralized MSE balancing design. $d = 15$ meters, $L = 2$, $K = 3$, $\varepsilon_{\text{m}} = 0.6$, $P_{\text{int}} = 3$ dB, $P_{\text{max,m}} = 40$ dB, and $P_{\text{max,f}} = 10$ dB and 15 dB for two cases: (a) Equal HU QoS priority ($\varepsilon_{\text{f},1} = \varepsilon_{\text{f},2} = \varepsilon_{\text{f},3} = 0.6$) and (b) unequal HU QoS priority ($\varepsilon_{\text{f},1} = 0.6$, $\varepsilon_{\text{f},2} = 0.7$, $\varepsilon_{\text{f},3} = 0.8$).

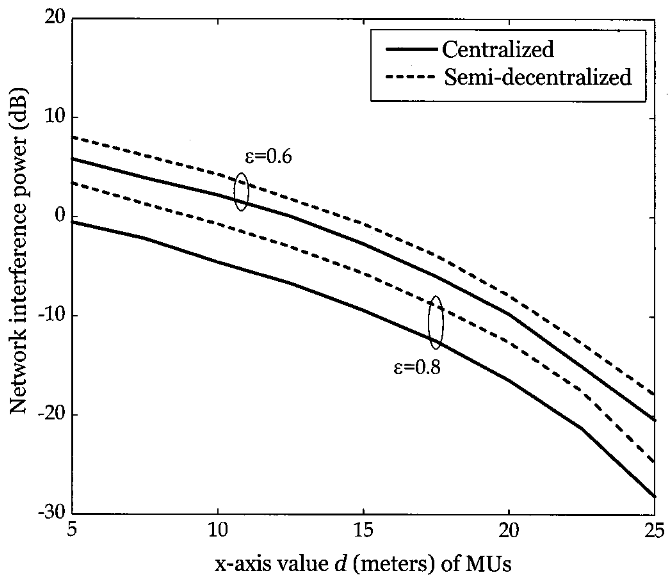

Fig. 7. Network interference power for the centralized and semi-decentralized designs as a function of the x-axis value d (meters) of MUs. $\varepsilon = \varepsilon_{\text{m}} = \varepsilon_{\text{f}} = 0.6$ and 0.8, $P_{\text{max,m}} = 60$ dB, $P_{\text{max,f}} = 20$ dB, and $P_{\text{int}} = 3$ dB.

design in subsection V-A and the robust semi-decentralized design in subsection V-B as a function of the uncertainty ρ when $d = 10$ meters, $\varepsilon = \varepsilon_{\text{m}} = \varepsilon_{\text{f}} = 0.6$, and $P_{\text{int}} = 3$ dB for the robust semi-decentralized design. We can observe from the figure that our robust algorithm for the total transmit power minimization is operative in the presence of channel uncertainty. We also see that the required total transmit power increases with the amount of uncertainty, as expected.

Users' random locations: We consider random locations of MUs and HUs (see Fig. 9 for the realization example). The FAP and MBS are located at $(0, 0)$ and $(250, 250)$, respectively. The 4 HUs are randomly scattered over a 20 meters $\times$ 20 meters rectangular area, while the L MUs are randomly scattered over a hexagonal area of radius 500 meters. We set the near-far region limit at 2 meters around of each transmitter. Fig. 10 shows

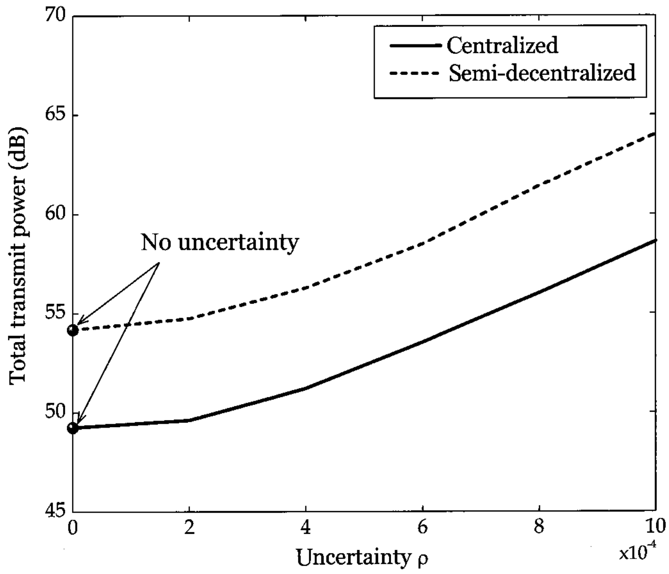

Fig. 8. Total transmit power for the robust centralized and the robust semi-decentralized designs as a function of the uncertainty ρ. $\rho = \delta_{\text{f},l} = \eta_{\text{m},k}$. $d = 10$ meters, $\delta_{\text{m},l} = \eta_{\text{f},k} = 0$, $\varepsilon = \varepsilon_{\text{m}} = \varepsilon_{\text{f}} = 0.6$, and $P_{\text{int}} = 3$ dB for the robust semi-decentralized design.

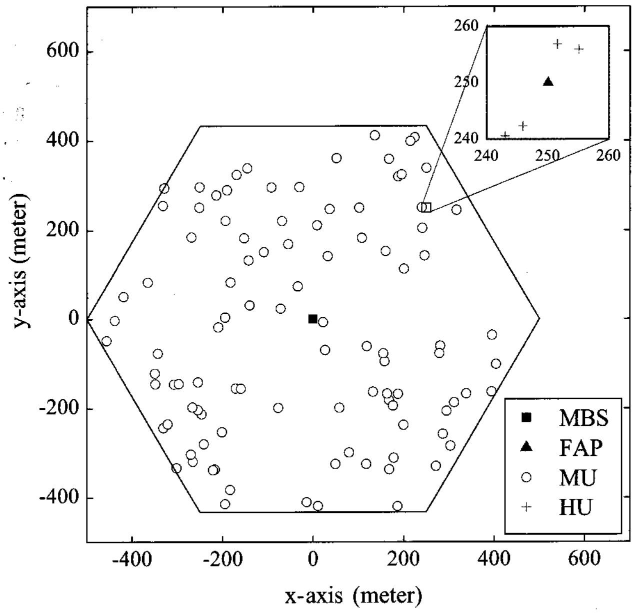

Fig. 9. An example realization for random locations of MUs and HUs. The FAP and MBS are located at $(0, 0)$ and $(250, 250)$, respectively. The 4 HUs are randomly scattered over a 20 meters $\times$ 20 meters rectangular area, while the 100 MUs are randomly scattered over a hexagonal area of radius 500 meters. We set the near-far region limit at 2 meters around each transmitter.

the required minimum transmit power for the centralized and the semi-decentralized designs versus the number of MUs L. In this example, we set the target SINRs for the MUs and HUs are -60 dB and -10 dB, respectively; and $P_{\text{int}} = 3$ dB for the semi-decentralized design. We use 5000 realizations for the simulation. As expected, the required minimum total transmit power increases with the number of MUs L for both designs in order to serve more users while guaranteeing QoS of each user.

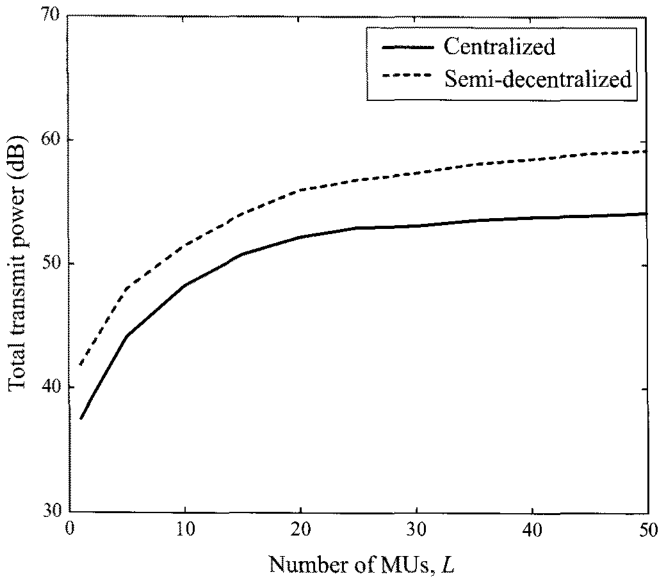

Fig. 10. Total transmit power for the centralized and the semi-decentralized designs versus the number of MUs L. The target SINRs for the MUs and HUs are -60 dB and -10 dB, respectively; and $P_{\rm int} = 3$ dB for the semi-decentralized design.

VII. CONCLUSION

In this paper, we considered the downlink two-tier MISO network comprising of the MBS and FAP serving multiple users. We formulated the following beamforming optimization problems: i) Total transmit power minimization problem; ii) MSE balancing problem; and iii) interference power minimization problem to ensure the user QoS for spectrum underlay. Using convex optimization techniques, we solved the beamforming optimization problems when a centralized controller and perfect global CSI are available. Since the centralized design is not always feasible in practice, we also proposed semi-decentralized algorithms to design the beamfomer and power allocation for the above optimization problems with only minimal information exchange between the transmitters. Taking into further account imperfect CSI, we extended our centralized and semi-decentralized beamforming design algorithms to robust versions using the worst-case design. Numerical results validated our proposed algorithms and demonstrated the effect of different system parameters on each optimization problem.

REFERENCES

[1] G. Staple and K. Werbach, "The end of spectrum scarcity," *IEEE Spectrum*, vol. 41, no. 3, pp. 49–52, Mar. 2004.

[2] D. López-Pérez, İ. Güvenc, G. de la Roche, M. Kountouris, T. Q. S. Quek, and J. Zhang, "Enhanced intercell interference coordination challenges in heterogeneous networks," *IEEE Commun. Mag.*, vol. 18, no. 3, pp. 22–30, June 2011.

[3] V. Chandrasekhar, J. G. Andrews, and A. Gatherer, "Femtocell networks: A survey," *IEEE Commun. Mag.*, vol. 46, no. 9, pp. 59–67, Sept. 2008.

[4] W. C. Chung, T. Q. S. Quek, and M. Kountouris, "Throughput optimization in two-tier femtocell networks," *IEEE J. Sel. Areas Commun.*, revised, July 2011.

[5] Y. Jeong, H. Shin, and M. Z. Win, "Optimum combining in femtocell networks," *IEEE J. Sel. Areas Commun.*, revised, July 2011.

[6] V. Chandrasekhar, J. G. Andrews, T. Muharemovic, Z. Shen, and A. Gatherer, "Power control in two-tier femtocell networks," *IEEE Trans. Wireless Commun.*, vol. 8, no. 8, pp. 4316–4328, Aug. 2009.

[7] O. Simeone, E. Erkip, and S. Shamai (Shitz), "Robust transmission and interference management for femtocells with unreliable network access," *IEEE J. Sel. Areas Commun.*, vol. 28, no. 9, pp. 1469–1478, Dec. 2010.

[8] V. Chandrasekhar and J. G. Andrews, "Uplink capacity and interference avoidance for two-tier femtocell networks," *IEEE Trans. Wireless Commun.*, vol. 8, no. 7, pp. 3498–3509, July 2009.

[9] ——, "Coverage in multi-antenna two-tier networks," *IEEE Trans. Wireless Commun.*, vol. 8, no. 10, pp. 5314–5327, Oct. 2009.

[10] M. Husso, J. Hämäläinen, R. Jäntti, J. Li, E. Mutafungwa, R. Wichman, Z. Zhend, and A. M. Wyglinski, "Interference mitigation by practical transmit beamforming methods in closed femtocells," *EURASIP J. Wireless Commun. and Networking*, vol. 2010, pp. 1–12, 2010, article ID 186815.

[11] D. Lopez-Pérez, A. Valcarce, G. de la Roche, and J. Zhang, "OFDMA femtocells: A roadmap on interference avoidance," *IEEE Commun. Mag.*, vol. 9, pp. 41–48, Sept. 2009.

[12] M. Yavuz, F. Meshkati, S. Nanda, A. Pokhariyal, N. Johnson, B. Raghothaman, and A. Richardson, "OFDMA femtocells: A roadmap on interference avoidance," *IEEE Commun. Mag.*, vol. 9, pp. 102–109, Sept. 2009.

[13] H. Shin and J. H. Lee, "Capacity of multiple-antenna fading channels: Spatial fading correlation, double scattering, and keyhole," *IEEE Trans. Inf. Theory*, vol. 49, no. 10, pp. 2636–2647, Oct. 2003.

[14] ——, "Performance analysis of space–time block codes over keyhole Nakagami-m fading channels," *IEEE Trans. Veh. Technol.*, vol. 53, no. 2, pp. 351–362, Mar. 2004.

[15] H. Shin, M. Z. Win, J. H. Lee, and M. Chiani, "On the capacity of doubly correlated MIMO channels," *IEEE Trans. Wireless Commun.*, vol. 5, no. 8, pp. 2253–2265, Aug. 2006.

[16] H. Shin and M. Z. Win, "MIMO diversity in the presence of double scattering," *IEEE Trans. Inf. Theory*, vol. 54, no. 7, pp. 2976–2996, July 2008.

[17] ——, "Gallager's exponent for MIMO channels: A reliability–rate tradeoff," *IEEE Trans. Commun.*, vol. 57, no. 4, pp. 972–985, Apr. 2009.

[18] F. Rashid-Farrokhi, K. J. R. Liu, and L. Tassiulas, "Transmit beamforming and power control for cellular wireless systems," *IEEE J. Sel. Areas Commun.*, vol. 16, no. 8, pp. 1437–1450, Oct. 1998.

[19] A. Wiesel, Y. C. Eldar, and S. Shamai (Shitz), "Linear precoding via conic optimization for fixed MIMO receivers," *IEEE Trans. Signal Process.*, vol. 54, no. 1, pp. 161–176, Jan. 2006.

[20] S. Shi, M. Schubert, and H. Boche, "Dowinlink MMSE transceiver optimization for multiuser MIMO systems: MMSE balancing," *IEEE Trans. Signal Process.*, vol. 56, no. 8, pp. 3702–3712, Aug. 2008.

[21] J. Yu, Y.-D. Yao, A. F. Molisch, and J. Zhang, "Performance evaluation of CDMA reverse links with imperfect beamforming in a multicell environment using a simplified beamforming model," *IEEE Trans. Veh. Technol.*, vol. 55, no. 3, pp. 1019–1031, May 2006.

[22] M. Sadek, A. Tarighat, and A. H. Sayed, "A leakage-based precoding scheme for downlink multi-user MIMO channels," *IEEE Trans. Wireless Commun.*, vol. 6, no. 5, pp. 1711–1721, May 2007.

[23] W. W. L. Ho, T. Q. S. Quek, S. Sun, and R. W. Heath Jr., "Decentralized precoding for multicell MIMO downlink," *IEEE Trans. Wireless Commun.*, vol. 10, no. 6, pp. 1798–1809, June 2011.

[24] H. Zhang, N. B. Mehta, A. F. Molisch, J. Zhang, and H. Dai, "Asynchronous interference mitigation in cooperative base station systems," *IEEE Trans. Wireless Commun.*, vol. 7, no. 1, pp. 155–165, Jan. 2008.

[25] Y. Ma, D. I. Kim, and Z. Wu, "Optimization of OFDMA-based cellular cognitive radio networks," *IEEE Trans. Commun.*, vol. 58, no. 8, pp. 2265–2276, Aug. 2010.

[26] Y. Ma and D. I. Kim, "Centralized and distributed optimization of ad-hoc cognitive radio network," in *Proc. IEEE GLOBECOM*, Honolulu, Hawaii, USA, Nov. 2009, pp. 1–7.

[27] S. A. Vorobyov, A. B. Gershman, and Z.-Q. Luo, "Robust adaptive beamforming using worst-case performance optimization: A solution to the signal mismatch problem," *IEEE Trans. Signal Process.*, vol. 51, no. 2, pp. 313–324, Feb. 2003.

[28] T. Q. S. Quek, H. Shin, and M. Z. Win, "Robust wireless relay networks: Slow power allocation with guaranteed QoS," *IEEE J. Select. Topics Signal Process.*, vol. 1, no. 4, pp. 700–713, Dec. 2007.

[29] A. Ben-Tal and A. Nemirovski, "Robust convex optimization," *Math. Oper. Res.*, vol. 21, no. 4, pp. 769–805, Nov. 1998.

[30] L. E. Ghaoui, F. Oustry, and H. Lebret, "Robust solutions to uncertain semidefinite programs," *SIAM J. Optim.*, vol. 9, no. 1, pp. 33–52, 1998.

[31] D. Guo, S. Shamai (Shitz), and S. Verdú, "Mutual information and minimum mean-square error in Gaussian channels," *IEEE Trans. Inf. Theory*, vol. 51, no. 4, pp. 1261–1282, Apr. 2005.

[32] M. Gruber, O. Blume, D. Ferling, D. Zeller, M. A. Imran, and E. C. Strinati, "EARTH - energy aware radio and network technologies," in *Proc. IEEE PIMRC*, Tokyo, JAPAN, Sept. 2009, pp. 1–5.

[33] S. Boyd and L. Vandenberghe, *Convex Optimization*. Cambridge, UK: Cambridge University Press, 2004.
[34] T. Q. S. Quek, M. Z. Win, and M. Chiani, "Robust power allocation algorithms for wireless relay networks," *IEEE Trans. Commun.*, vol. 58, no. 7, pp. 1931–1938, July 2010.
[35] J. Zander, "Performance of optimum transmitter power control in cellular radio systems," *IEEE Trans. Veh. Technol.*, vol. 41, no. 1, pp. 57–62, Feb. 1992.
[36] M. Bengtsson and B. Ottersten, *Optimal and Suboptimal Transmit Beamforming*. CRC Press, 2001.

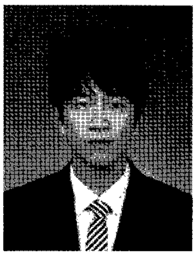

Youngmin Jeong received the B.E. and M.E. degrees in Electronics and Radio Engineering from Kyung Hee University, Yongin, Korea, in 2009 and 2011, respectively. He is currently working toward the Ph.D. degree in Electronics and Radio Engineering at Kyung Hee University. His current research interests include wireless communications, cooperative communications, and heterogeneous networks.

Tony Q. S. Quek received the B.E. and M.E. degrees in Electrical and Electronics Engineering from Tokyo Institute of Technology, Tokyo, Japan, in 1998 and 2000, respectively. At Massachusetts Institute of Technology (MIT), Cambridge, MA, he earned the Ph.D. in Electrical Engineering and Computer Science in Feb. 2008. Since 2008, he has been with the Institute for Infocomm Research, A*STAR, where he is currently a Principal Investigator and Scientist. His main research interests are the application of mathematical, optimization, and statistical theories to communication, detection, information theoretic and resource allocation problems. Specific current research topics include cooperative networks, smart grid, interference networks, heterogeneous networks, green communications, wireless security, and cognitive radio. He has been actively involved in organizing and chairing sessions, and has served as a Member of the Technical Program Committee (TPC) in a number of international conferences. He served as the Technical Program Chair for the Services & Applications Track for the IEEE Wireless Communications and Networking Conference (WCNC) in 2009, the Cognitive Radio & Cooperative Communications Track for the IEEE Vehicular Technology Conference (VTC) in Spring 2011, and the Wireless Communications Symposium for the IEEE Globecom in 2011; as Technical Program Vice-Chair for the IEEE Conference on Ultra Wideband in 2011; and as the Workshop Chair for the IEEE Globecom 2010 Workshop on Femtocell Networks and the IEEE ICC 2011 Workshop on Heterogeneous Networks. He is currently an Editor for the Wiley Journal on Security and Communication Networks and the European Transactions on Telecommunications. He was Guest Editor for the Journal of Communications and Networks (Special Issue on Heterogeneous Networks) in 2011. He received the Singapore Government Scholarship in 1993, Tokyu Foundation Fellowship in 1998, and the A*STAR National Science Scholarship in 2002. He was honored with the 2008 Philip Yeo Prize for Outstanding Achievement in Research, the IEEE Globecom 2010 Best Paper Award, and the 2011 JSPS Invited Fellow for Research in Japan.

Hyundong Shin received the B.S. degree in Electronics Engineering from Kyung Hee University, Korea, in 1999, and the M.S. and Ph.D. degrees in Electrical Engineering from Seoul National University, Seoul, Korea, in 2001 and 2004, respectively. From September 2004 to February 2006, he was a Postdoctoral Associate at the Laboratory for Information and Decision Systems (LIDS), Massachusetts Institute of Technology (MIT), Cambridge, MA, USA. In 2006, he joined Kyung Hee University, Korea, where he is now an Assistant Professor at the Department of Electronics and Radio Engineering. His research interests include wireless communications and information theory with current emphasis on MIMO systems, cooperative and cognitive communications, network interference, vehicular communication networks, and intrinsically secure networks. He has served as a Member of the Technical Program Committee (TPC) in a number of international conferences. He served as the Technical Program Co-chair for the PHY Track of the IEEE Wireless Communications and Networking Conference (WCNC) in 2009 and the Communication Theory Symposium of the IEEE Global Communications Conference (Globecom) in 2012. He is currently an Editor for the IEEE Transactions on Wireless Communications and the KSII Transactions on Internet and Information Systems. He was a Guest Editor for the EURASIP Journal on Advances in Signal Processing (Special Issue on Wireless Cooperative Networks) in 2008. He was honored with the Knowledge Creation Award in the field of Computer Science from Korean Ministry of Education, Science and Technology in 2010. He received the IEEE Communications Society's Guglielmo Marconi Best Paper Award in 2008, the IEEE Vehicular Technology Conference (VTC) Best Paper Award in Spring 2008, and the IEEE VTS APWCS Best Paper Award in 2010.